

A COMPARISON OF THE BIORID II, HYBRID III, AND RID2 IN LOW-SEVERITY REAR IMPACTS

A. Kim
A. Sutterfield
A. Rao
K.F. Anderson
J. Berliner
J. Hassan
A. Irwin
J. Jensen
J. Kleinert
H.J. Mertz
H. Pietsch
S. Rouhana
R. Scherer

Rear Impact Dummy Evaluation Task Group of the
Occupant Safety Research Partnership/USCAR
United States of America
Paper Number 05-0225

ABSTRACT

The BioRID II, 50th percentile Hybrid III and RID2 crash test dummies, all representing a mid-size adult male, were subjected to HyGE™ rear impact sled tests. Their measured and calculated responses were used to evaluate their sensitivity to sled velocity, head restraint position, and other test setup parameters. Three test series were conducted using different sled acceleration pulses and different types of seats. For conditions where three identical tests were conducted, repeatability was evaluated. In Series A, the effect of sled velocity on the Hybrid III and RID2 was evaluated. For the RID2, the effect of the initial backset was also evaluated in this series. In Series B, the head restraint position and the sled velocity were changed to see how the performances of the BioRID II, Hybrid III and RID2 were affected. In Series C, the effect of sled velocity changes and head restraint position on the Hybrid III and RID2 were again evaluated, and repeatability was assessed. Comments on the handling and durability of the dummies are also provided.

INTRODUCTION

The Occupant Safety Research Partnership (OSRP) of the United States Council for Automotive

Research (USCAR) evaluated the BioRID II (version C), the Hybrid III (FMVSS Part 572 Subpart E), and the RID2 (a prototype representative of production version 0.0). All three dummies represent the mid-size adult male. The Hybrid III was developed in the early 1970s [9, 21]. Although it has primarily been used in frontal impacts, it has also been used in rear, side and other types of impacts. Both the BioRID II [2, 7] and the RID2 [15] were developed more recently and were intended specifically for use in low-severity rear impacts.

In this study, the similarities and differences between these dummies were evaluated as well as the way each dummy was affected by changes in the test parameters. Three different test series were run in this evaluation. Series A examined the sensitivity to changes in sled velocity of the Hybrid III and RID2 when set to the same backset (the horizontal distance between the back of each dummy's head and the front the head restraint). The effect of varying the backset on the responses of the RID2 was also evaluated. In Series B, the effect of sled velocity and head restraint position on the responses of the Hybrid III, RID2 and BioRID II were evaluated. Additionally, the effect of varying the backset on the BioRID II was assessed. Series C further examined the sensitivity of the Hybrid III and RID2 to sled velocity and head restraint position and analyzed the repeatability of each dummy.

Each of the three different series of rear impact HyGE™ sled tests was run at a different test laboratory. The test matrix is shown in Table 1. The sled velocities ranged from 9 to 27 km/hr.

METHODS

General Setup

All the dummies were dressed consistently throughout the entire evaluation. The BioRID II was dressed in two pairs of shirts and shorts. The inner pair was made of Lycra® and the outer pair was made of cotton. The Hybrid III wore a cotton shirt and shorts. The RID2 was dressed in the provided neoprene suit.

Table 1.
Test Matrix

Test Series	ΔV (km/hr)	Dummies	Position	Head Restraint Position	# of Tests Per Dummy
A	9	Hybrid III, RID2, RID2 (105mm)	Driver	Fixed	1,1,1
A	9	Hybrid III, RID2, RID2 (105mm)	Passenger	Fixed	1,1,1
A	16	Hybrid III, RID2, RID2 (105mm)	Driver	Fixed	1,1,1
A	16	Hybrid III, RID2, RID2 (105mm)	Passenger	Fixed	1,1,1
A	24	Hybrid III, RID2, RID2 (105mm)	Driver	Fixed	1,1,1
A	24	Hybrid III, RID2, RID2 (105mm)	Passenger	Fixed	1,1,1
B	17	RID2, Hybrid III, BioRID II	Fore, Mid, Aft	Full Up	2,2,2
B	17	RID2, Hybrid III, BioRID II	Fore, Mid, Aft	Full Down	2,2,2
B	27	RID2, Hybrid III, BioRID II	Fore, Mid, Aft	Full Up	2,2,2*
B	27	RID2, Hybrid III, BioRID II	Fore, Mid, Aft	Full Down	2,2,2
C	10	Hybrid III, RID2	Driver	Full Up	1,2
C	10	Hybrid III, RID2	Passenger	Full Up	2,1
C	10	Hybrid III, RID2	Driver	Full Down	1,2
C	10	Hybrid III, RID2	Passenger	Full Down	2,1
C	24	Hybrid III, RID2	Driver	Full Up	1,2
C	24	Hybrid III, RID2	Passenger	Full Up	2,1
C	24	Hybrid III, RID2	Driver	Full Down	1,2
C	24	Hybrid III, RID2	Passenger	Full Down	2,1

* Only one of the BioRID II, 27 km/hr ΔV head restraint full up tests is included in the dummy comparison discussion for test Series B due to positioning issues.

The three facilities also used a standard set of minimum instrumentation for each dummy as listed in Table 2. The BioRID II used in this evaluation was not instrumented with a lower neck load cell. The transducers were oriented and the responses were filtered according to SAE J211 convention [19]. The dummies passed verification before and after each test series. The test facilities recorded the simulated rear impacts with high-speed film cameras at 500 and 1000 frames/second.

Table 2.
Dummy Instrumentation

	BioRID II	Hybrid III	RID2
Head CG 3-axis accelerometer	*	*	*
Upper neck 6-axis load cell	*	*	*
Lower neck 6-axis load cell		*	*
T1 single-axis (X) accelerometer		*	
T1 3-axis accelerometer	*		*

All the dummies were tested on production representative seats mounted to either a rigidized vehicle buck or a rigid platform buck. Each test series used a different type of seat. The dummies were restrained by 3-point safety belts in all the tests. The BioRID II and RID2 were positioned as recommended in their respective user manuals [2, 15]. The Hybrid III was positioned according to the FMVSS 208 seating procedure [8]. For each test, the backset was measured. The vertical height from the top of the head restraint to the center of gravity (CG) of the head was also measured. See Figure 1.

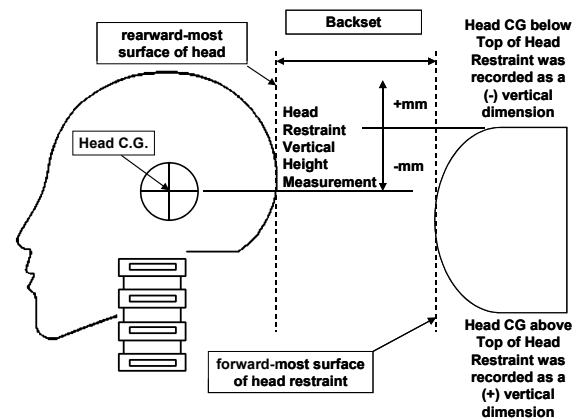


Figure 1. Head to head restraint backset and vertical height measurements.

The distances, formulas and methods for the following calculated responses are given in Appendix A. The external head impact forces were used to determine the contact forces with the head restraint. The tension-extension component of the Nij [13, 14, 1, 11, 12] and the NIC [23, 3, 4] were also evaluated.

The head restraint contact times were obtained by using a slope intercept approach, similar to the one described in SAE J2052 [20], on the external head impact force responses. The intercept value was calculated by taking the slope over a change of 50 N and extrapolating backwards to the point in time where the force level was zero.

Series A

In this test series, the Hybrid III and RID2 were subjected to simulated rear impacts with approximate sled velocity changes (ΔV s) of 9, 16, and 24 km/hr (Table 1). The sled acceleration pulses for each tested velocity are shown in Figure 2. The dummies were tested on identical bucket seats with integrated head restraints (Figure 3). The seats were replaced after each test. The seats were placed in the full rear seat track position. The seatbacks were set at 23°, measured between the seat frame and the vertical. The seating positions of the two dummies were switched from driver to passenger, and vice versa, for the repeat run of each test condition.

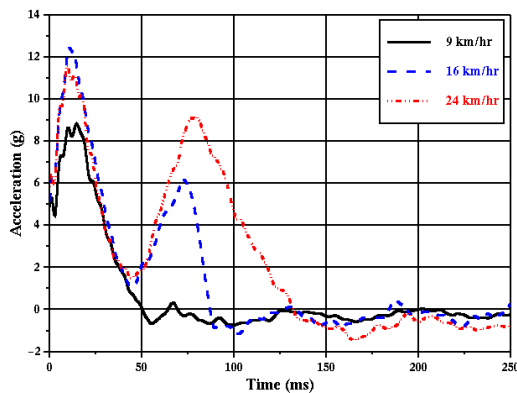


Figure 2. Series A: Sled acceleration pulses.

In its initial position, the Hybrid III backset was 55 mm. When the RID2 was first positioned according to its procedure [15], an average backset of 105 mm was obtained. In later tests using the same seating procedure, the RID2 was repositioned to match the 55 mm backset of the Hybrid III. Both dummies were positioned to the same H-point.

Figures 4 and 5 show the average and range of the backsets and the vertical distances from the center of gravity of the head to the top of the head restraint obtained for each test condition. The values obtained when the RID2 was at the 105 mm backset are labeled as "RID2 (105)". The RID2 initial setup tilt sensor readings are given in Appendix B Tables B1 and B2.



Figure 3. Series A: Test setup at 55 mm backset. Foreground – RID2, background – Hybrid III.

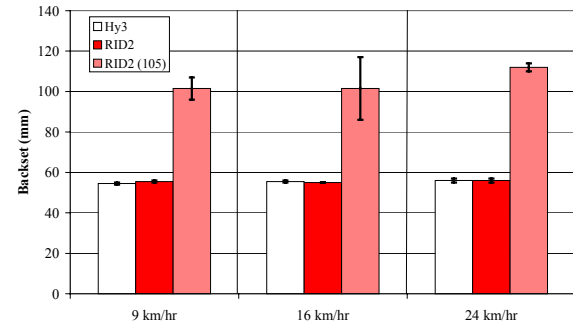


Figure 4. Series A: Backsets.

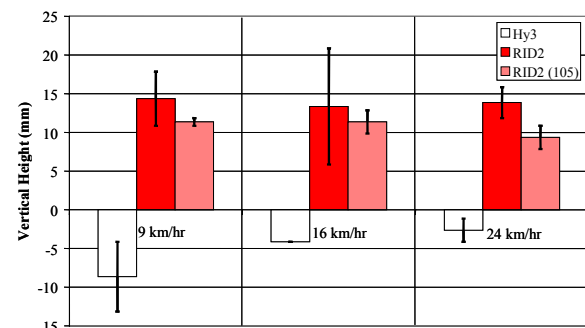


Figure 5. Series A: Vertical heights between the top of the head restraint and the head CG.

Series B

In the second test series, the Hybrid III, RID2 and BioRID II were tested concurrently (Figure 6) at ΔV s of 17 and 27 km/hr as shown in Table 1. The sled acceleration pulses are shown in Figure 7. Identical front bucket passenger seats with integrated 3-point belts were used and replaced after each test. The seats had adjustable head restraints and were also equipped with actuation devices that controlled head restraint movement (self-aligning head restraint mechanisms). The initial positions of the head restraints were either full up or full down. The seatbacks were set at an approximate angle of 16° .

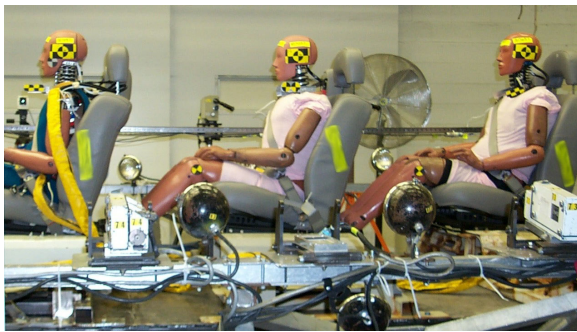


Figure 6. Series B: Test setup. From left-to-right, the RID2, Hybrid III, and BioRID II.

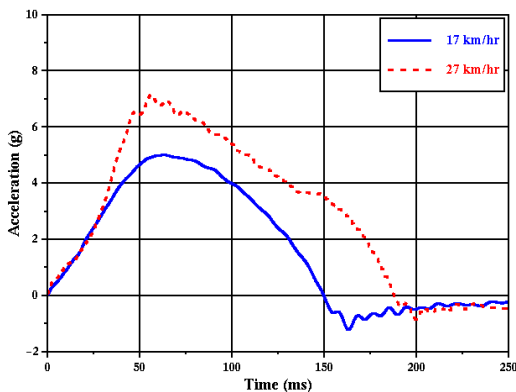


Figure 7. Series B: Sled acceleration pulses.

Figure 8 gives the average and range of the backsets for each test condition. The averages and ranges of the vertical heights from the top of the head restraint to the head CG, obtained by film analysis, are given in Figure 9. The RID2 tilt sensor angles at initial position are listed in Appendix B Table B3.

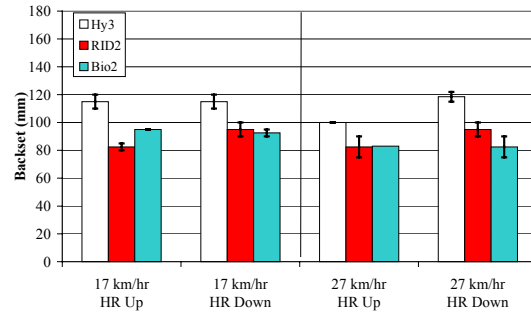


Figure 8. Series B: Backsets.

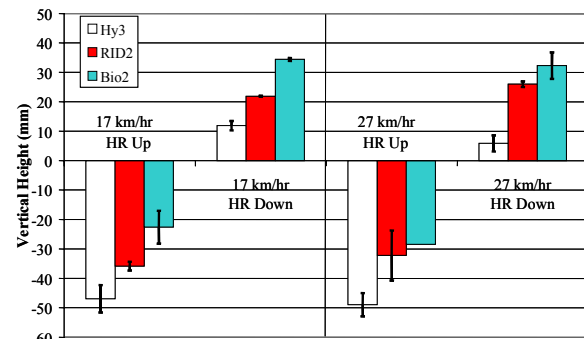


Figure 9. Series B: Vertical heights between the top of the head restraint and the head CG.

Series C

In the third series, a total of 12 sled tests were conducted with the Hybrid III and RID2 dummies (Figure 10). The sled tests were conducted at ΔV s of 10 and 24 km/hr (Table 1). Figure 11 shows the sled pulses used in this series. Identical front bucket seats with integrated 3-point belts were used. The same set of driver and passenger seats were used for the 10 km/hr tests, however, new seats were used for each of the 24 km/hr tests. The seats had adjustable head restraints that were set at either the full up or full down position. The seatbacks were set at an angle of 24° .

The dummies were seated side by side in bucket seats and their positions were switched in some of the tests (Table 1). Figure 12 gives the average and the range of backsets. From still setup photographs (Figure 13), it was observed that the tops of the head restraints in both the full up and full down positions were always above the CGs of the heads of the two dummies. This behavior was also seen for the RID2 in the 24 km/hr test setup. The initial RID2 angles are given in Appendix B Table B4.

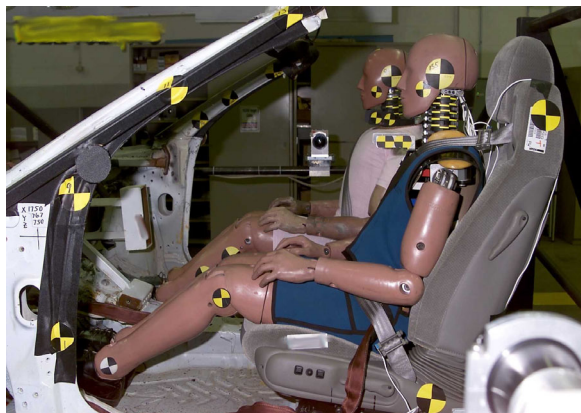


Figure 10. Series C: Test setup. Foreground - RID2, background - Hybrid III.

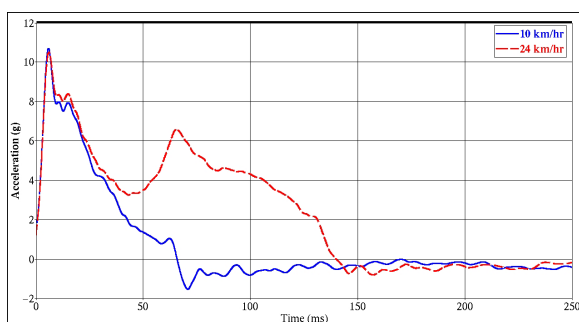


Figure 11. Series C: Sled acceleration pulses.

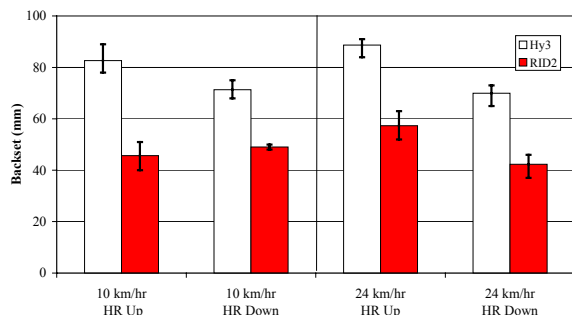


Figure 12. Series C: Backsets.

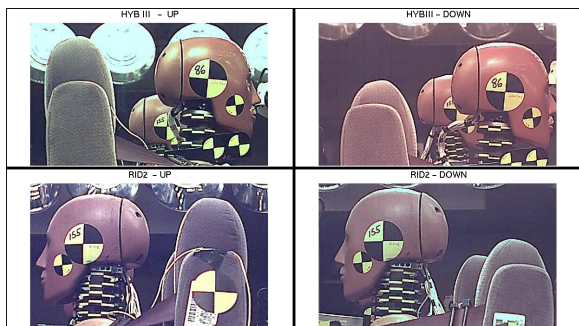


Figure 13. Test setup photographs. Top left - Hybrid III HR up, top right - Hybrid III HR down, bottom left - RID2 HR up, bottom right - RID2 HR down.

RESULTS AND DISCUSSION

The results of each test series are first discussed individually. Then, any observations that can be made by comparing two or more of the series are given. Lastly, there are comments on dummy handling and usability.

All bar chart graphs have the following format. Each bar represents the average of the peak responses for that test condition while the error bars represent the ranges.

Series A

This series examined the sensitivity of the Hybrid III and RID2 to sled velocity when both dummies were set to the same backset. Due to the difference in dummy seated heights, the effect of height was also indirectly observed. Although the following charts (e.g. Figure 14) show data for the Hybrid III, RID2, and RID2(105) only the Hybrid III and RID2 data will be discussed in the 55 mm Backset section. The RID2(105) data will be discussed in a later section on RID2 backset sensitivity.

55 mm Backset: Hybrid III and RID2

Resultant Head CG Accelerations

The averages of the peak head CG accelerations, obtained prior to the head losing contact with the head restraint due to rebound, are shown in Figure 14. The Hybrid III and RID2 have very similar peak resultant head CG accelerations. The average peak accelerations of both dummies increased between 9 and 16 km/hr but not between 16 and 24 km/hr. The increased seatback deformation seen at 24 km/hr (Figure 15), compared to that seen at 16 km/hr, limited the effect of this sled velocity increase on the head CG accelerations.

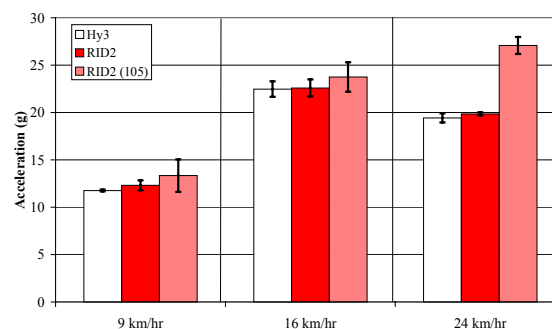
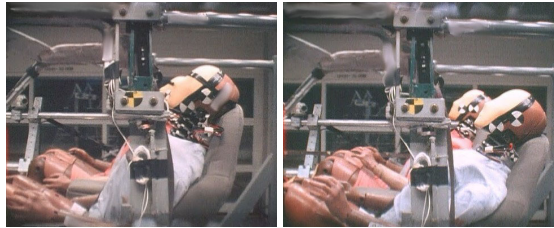


Figure 14. Series A: Resultant head CG accelerations.



a.) b.)
Figure 15. Series A: Maximum seatback deformation with a Hybrid III a.) 16 km/hr and b.) 24 km/hr.

T1 X-Accelerations

At each sled velocity, the average peak T1 X-accelerations of the Hybrid III and RID2 were within 2 g of each other (Figure 16). The peak accelerations of both dummies increased from 9 to 16 km/hr. At 24 km/hr, seatback deformation again limited the responses. The largest increase seen at this level was less than 1.5 g.

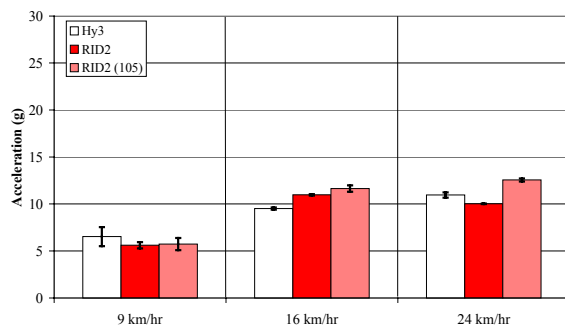


Figure 16. Series A: T1 X-accelerations.

Upper Neck Shear Forces

At 9 and 24 km/hr, the peak upper neck shear forces of the Hybrid III were greater than those of the RID2 (Figure 17). However, at 16 km/hr the peak responses of the dummies were similar. Due to the seatback deformation at 24 km/hr, the peak upper neck shear forces only increased between 9 and 16 km/hr.

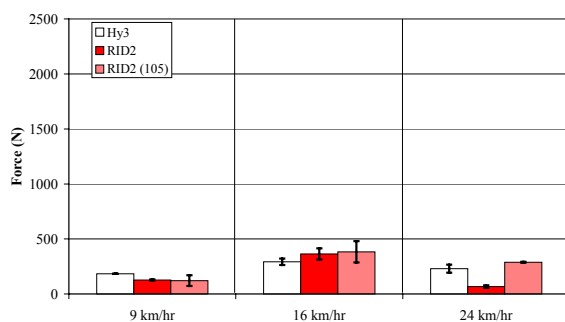


Figure 17. Series A: Upper neck shear forces, Fx.

Lower Neck Shear Forces

The Hybrid III and RID2 peak lower neck shear forces were comparable at each sled velocity (Figure 18). The lower neck shear forces of both dummies increased from 9 to 16 km/hr, but not at 24 km/hr. Like the upper neck shear forces, the seatback deformation occurring at this speed minimized the effect of the sled velocity increase on these responses. For both dummies, the shear forces at the lower neck were at least 35% greater than those at the upper neck.

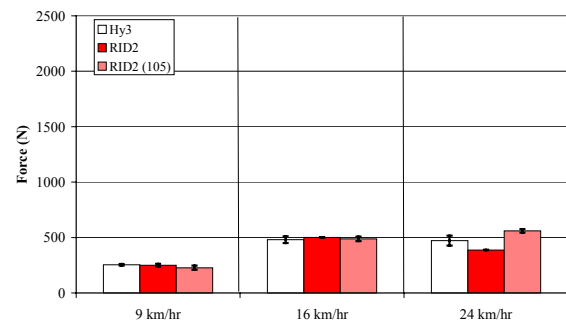


Figure 18. Series A: Lower neck shear forces, Fx.

Upper Neck Tensile Forces

In the axial direction, the peak RID2 upper neck forces were consistently greater than those of the Hybrid III (Figure 19). This is explained by the different seated heights of the two dummies. The head of the RID2, which had the greater seated height (Figure 5), hit higher on the head restraint than the Hybrid III. This resulted in the RID2 stretching over the head restraint more than the Hybrid III, resulting in higher tensile forces. The RID2 upper neck axial forces were more than double its respective shear forces. At 16 and 24 km/hr, the Hybrid III upper neck axial forces were also more than double its shear forces. The Hybrid III peak tensile responses increased with sled velocity across the entire range while those of the RID2 only increased from 9 to 16 km/hr. With respect to upper neck tension, the seatback deformation seen at 24 km/hr only limited the RID2's responses.

Lower Neck Tensile Forces

In general, the lower neck tensile forces of both dummies followed the behavior of their upper neck tensile forces. The RID2 lower neck tensile forces were consistently greater than those of the Hybrid III (Figure 20). At the lower neck, the RID2 axial forces were again more than double its respective shear forces; however, the Hybrid III axial forces were only greater than its shear forces at 24 km/hr. The Hybrid III peak tensile forces increased with each

increase in sled velocity, however, the RID2 forces only increased from 9 to 16 km/hr.

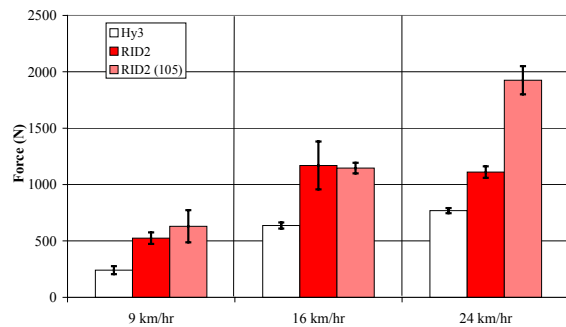


Figure 19. Series A: Upper neck tensile forces, Fz.

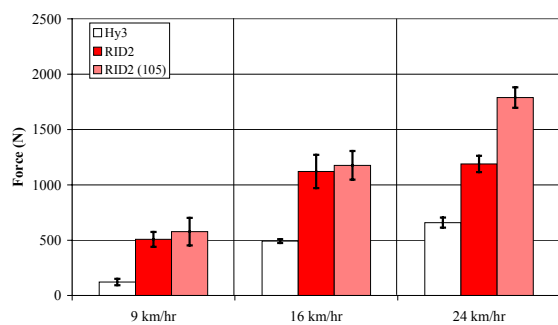


Figure 20. Series A: Lower neck tensile forces, Fz.

Occipital Condyle Extension Moments

The average extension moments at the occipital condyles are shown in Figure 21. Although the average Hybrid III extension moments were more than double those of the RID2 at each tested sled velocity, it should be noted that all the moments were less than 8 Nm. The differences between the dummies' responses were attributed to the lower bending stiffness of the RID2 neck [10].

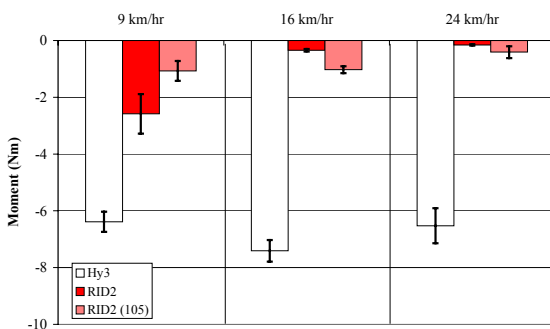


Figure 21. Series A: Occipital condyle extension moments, -My. (Note: The y-axis scale differs from that of Figure 22.)

C7/T1 Extension Moments

At the C7/T1 joint, the Hybrid III extension moments were approximately four times those of the RID2 (Figure 22). The lower bending stiffness of both the RID2 neck and thoracic spine, in comparison to the Hybrid III, contributed to this behavior [10]. The moments of both dummies increased from 9 to 16 km/hr, but it should be noted that the RID2 average moment only increased by 4 Nm. For the Hybrid III, the peak C7/T1 extension moments were at least five times greater than its occipital condyle moments.

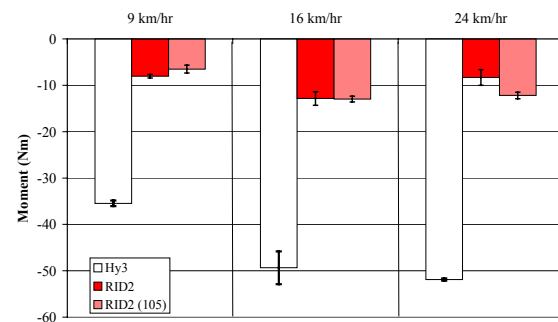


Figure 22. Series A: C7/T1 extension moments, -My. (Note: The y-axis scale differs from that of Figure 21.)

External Head Impact Fx Forces

The external head Fx forces were calculated and are shown in Figure 23. At the two lower sled velocities, the Hybrid III and RID2 responses were slightly different from each other. At 24 km/hr, the average Fx force of the RID2 was greater than that of the Hybrid III. The responses of both dummies increased from 9 to 16 km/hr. Again, the seatback deformation at 24 km/hr limited the effect of this increased sled velocity. At all three tested sled velocities, the RID2 neck also contacted the seat after initial head contact occurred. With the Hybrid III, this only occurred at the two higher velocities (16 and 24 km/hr).

External Head Impact Fz Forces

The RID2 external head Fz forces were greater than those of the Hybrid III (Figure 24). As with the upper neck tensile forces, this was due to the taller seated height of the RID2, which produced a different dummy to head restraint interaction. At 16 and 24 km/hr, the RID2 Fz forces had greater magnitudes than their corresponding Fx forces although the difference was less pronounced at the higher sled velocity. The peaks of both dummies increased from 9 to 16 km/hr. There were no

increases in the force responses when the sled velocity was increased to 24 km/hr.

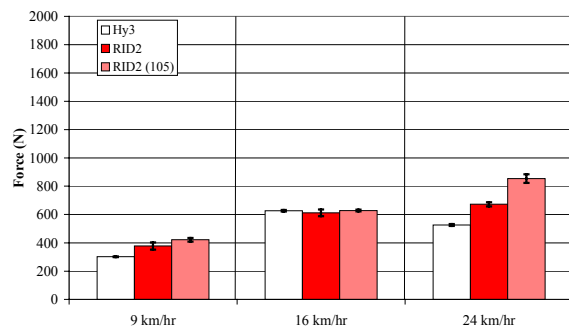


Figure 23. Series A: External head impact forces, Fx.

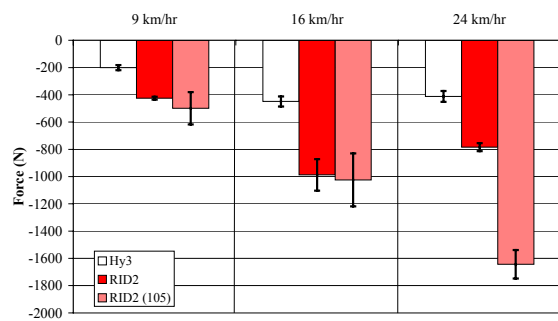


Figure 24. Series A: External head impact forces, Fz.

Head Restraint Contact Times

At 9 and 16 km/hr, the ranges of head restraint contact times for the Hybrid III and RID2 overlapped each other (Figure 25). Therefore, they were not considered to be different. At 24 km/hr, the ranges for each dummy were reduced, however the difference between the contact times of both dummies was no larger than it was at 16 km/hr. Neither the contact times of the Hybrid III nor those of the RID2 increased with sled velocity. One possible factor for this is that the dummies' interaction with the seat as the sled velocity was increased, caused more seatback deformation prior to contact. This would move the head restraint further rearward of the dummy's head, offsetting the effect of the increased sled velocity. Another factor may be the similarity of the sled acceleration pulses (Figure 2). All the pulses have very similar slopes, especially their onset slopes, and the dummies may be reacting the same way until they contact the head restraint.

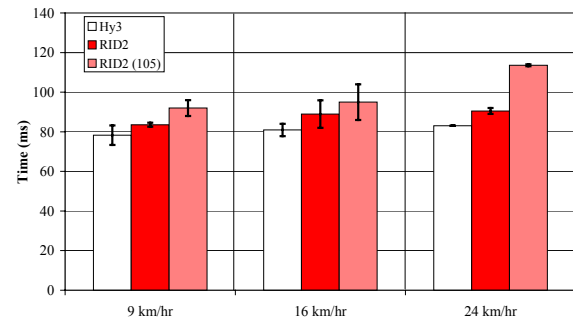


Figure 25. Series A: Head restraint contact times.

NICs

The average NIC values [23, 3, 4] of both dummies were equivalent at 9 km/hr as shown in Figure 26. At 16 and 24 km/hr, the RID2 average NICs were greater than those of the Hybrid III. Both the Hybrid III and the RID2 NIC values increased from 9 to 16 km/hr. At 24 km/hr, the effect of the sled velocity increase was countered by the effect of the seatback deformation and the NIC values did not increase.

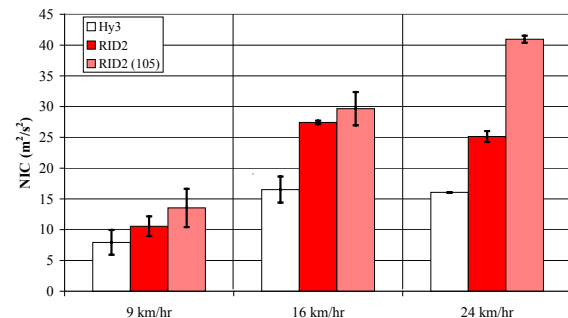


Figure 26. Series A: NICs.

Nij: Ntes

The average Nte values are shown in Figure 27. In this series, the Nte values were dominated by their tensile components. Since the RID2 had much higher tensile neck forces than the Hybrid III, due to its greater seated height, it also had greater Nte values. The Hybrid III Nte averages increased across the entire sled velocity range, while the RID2 Nte averages only increased from 9 to 16 km/hr. For the Nte, the seatback deformation that occurred at 24 km/hr limited the RID2's response but not the Hybrid III's response.

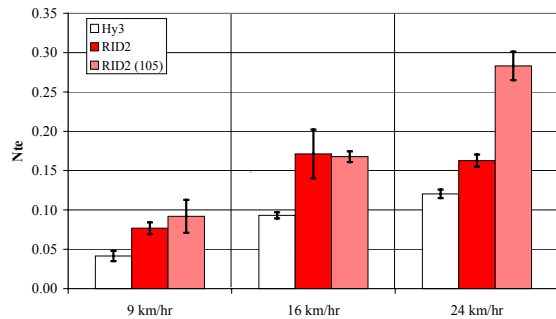


Figure 27. Series A: Ntes.

Seated Height

When set to the same backset of 55 mm, the RID2 sat higher than the Hybrid III with respect to the head restraint (Figure 5). This produced different kinematics. The Hybrid III initially struck the top front corner of the head restraint with the rear portion of its skullcap (Figure 28a). The RID2 initially struck the top of the head restraint more towards the bottom corner of its skullcap. The worst case is shown in Figure 28b. As a result, the RID2 stretched over the head restraint more and had greater axial forces (upper and lower neck tensile forces and external head impact Fz) than the Hybrid III.

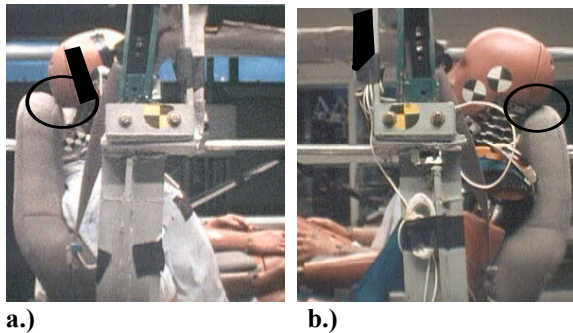


Figure 28. Series A: Initial contact, 55 mm backset and 16 km/hr ΔV, a.) Hybrid III and b.) RID2.

RID2: Backset Sensitivity

As can be seen from Figures 14 through 27, the majority of the RID2 responses, including head restraint contact time, were insensitive to the backset change from 55 to 105 mm at 9 and 16 km/hr. However, at 24 km/hr, both the measured and calculated RID2 responses increased at the larger backset. As previously stated, more seatback deformation occurs at this velocity than at 16 km/hr (Figure 15). This, in addition to the larger backset of 105 mm, delayed the head restraint contact time by approximately 13 ms (Figure 25) allowing the head to head restraint contact velocity to increase. At approximately 123 ms, the head struck the internal

head restraint structure as indicated by the resultant external head impact force time-history traces (Figure 29). This resulted in the magnitude increases noted previously and caused many of the responses to increase with sled velocity across the entire tested range of 9-24 km/hr, rather than just between 9 and 16 km/hr. Five of these responses have been normalized by their respective values at the 55 mm backset and are shown in Figure 30.

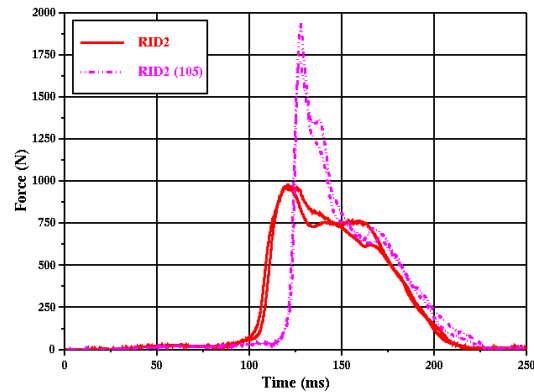


Figure 29. Series A: RID2 resultant external force time history curves, 24 km/hr ΔV.

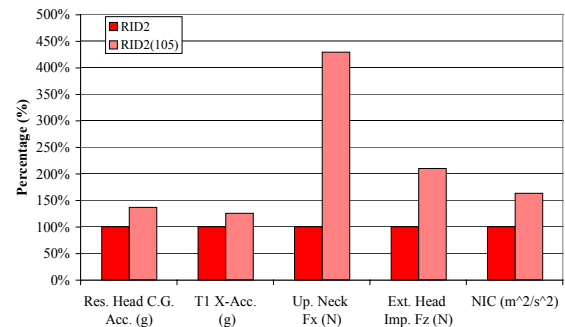


Figure 30. Series A: RID2 backset sensitivity, 24 km/hr. Normalized responses.

SERIES B

The responses of the RID2, the Hybrid III and the BioRID II in sled test Series B are compared in the following section. Each dummy was evaluated for its ability to differentiate between sled velocity (17 km/hr or 27 km/hr) and head restraint position (full up or full down). Two repeats of each test configuration were run. However, one of the BioRID II repeat tests was not used in the dummy comparison due to backset variance (see Table 1). These data were used to evaluate the BioRID II's sensitivity to backset. It should also be noted that the BioRID II version tested in this evaluation could not be

instrumented with a lower neck load cell. Therefore, it is not discussed in the lower neck response sections.

Resultant Head CG Accelerations

At 27 km/hr, the Hybrid III peak head acceleration was greater than that of the BioRID II, which in turn was greater than the RID2 value (Figure 31). At 17 km/hr, the dummy peak head accelerations were more similar. In all cases, the peaks increased with sled velocity. Similarly, the peaks increased as the head restraint position was changed from full up to full down. However, for the BioRID II at 27 km/hr, the difference between the two head restraint conditions was only 1.4 g.

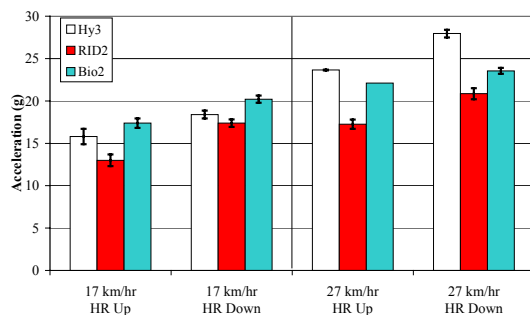


Figure 31. Series B: Resultant head CG accelerations.

T1 X-Accelerations

As shown in Figure 32, the Hybrid III peak T1 X-acceleration was consistently higher than the RID2 peak, however at 17 km/hr with the head restraint up, the difference was less than 1 g. All dummies increased peak T1 acceleration with increased sled velocity. Head restraint position did not influence the T1 X-accelerations.

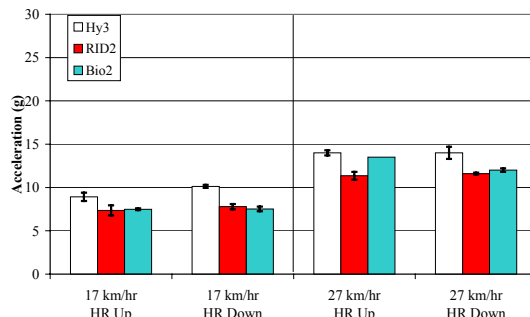


Figure 32. Series B: T1 X-accelerations.

Upper Neck Shear Forces

The Hybrid III peak upper neck shear forces were greater than those of the RID2 (Figure 33). This was due to the greater shear stiffness of the Hybrid III's neck [10] and its larger backsets. The Hybrid III peak upper neck shear forces were also greater than those of the BioRID II in the head restraint full up condition. At 27 km/hr with the head restraint full down, the BioRID II peak was greater than the RID2 and Hybrid III peaks. With respect to sled velocity, only the upper neck shear force of the BioRID II with the head restraint down increased from 17 to 27 km/hr. Only the BioRID II responses at 27 km/hr increased when the head restraint was moved from full up to full down.

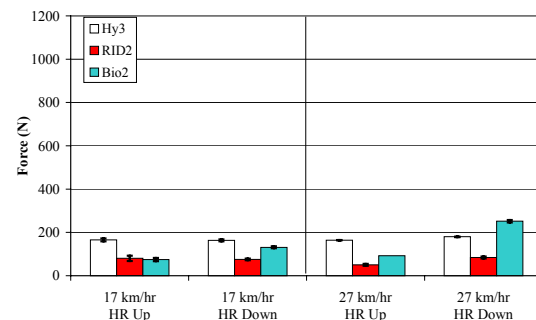


Figure 33. Series B: Upper neck shear forces, Fx.

Lower Neck Shear Forces

Similar to the upper neck shear forces, the lower neck shear forces of the Hybrid III were greater than those of the RID2 (Figure 34). This was due to the greater stiffness of the Hybrid III thoracic spine compared to that of the RID2 [10]. Only the Hybrid III responses and the RID 2 with the head restraint down increased consistently with sled velocity. Both the Hybrid III and RID2 responses increased as the head restraint was changed from up to down. For these two dummies, the peak lower neck shear forces were at least 2.5 times greater than the upper neck shear forces.

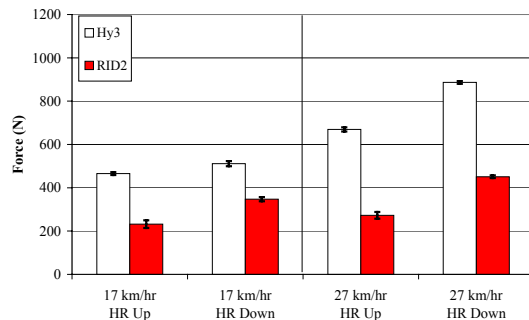


Figure 34. Series B: Lower neck shear forces, Fx.

Upper Neck Tensile Forces

The peak upper neck tensile forces of the BioRID II were greater than those of the Hybrid III and the RID2 except at 27 km/hr with the head restraint down, where all three dummies had similar peak values (Figure 35). At 17 km/hr with the head restraint down and 27 km/hr with the head restraint up, the Hybrid III peak was also greater than the RID2 peak. For all the dummies, the peak upper neck tension increased with the increase in sled velocity. Similarly, all dummies measured a higher peak upper neck tension when the head restraint position was full down. The peak upper neck tensile forces ranged from twice to nearly ten times that of their respective upper neck shear forces.

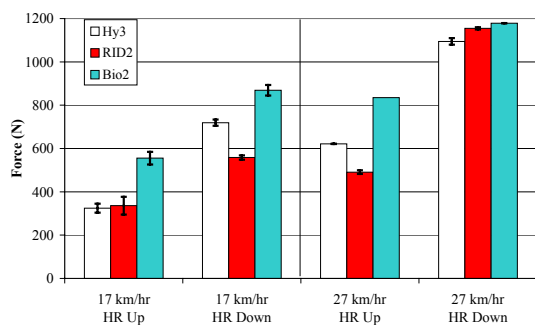


Figure 35. Series B: Upper neck tensile forces.

Lower Neck Tensile Forces

Figure 36 shows that the peak lower neck tensile forces of the RID2 were consistently greater than those of the Hybrid III. Additionally, the peak lower neck tension of both dummies increased with sled velocity and when the head restraint was lowered to the full down position.

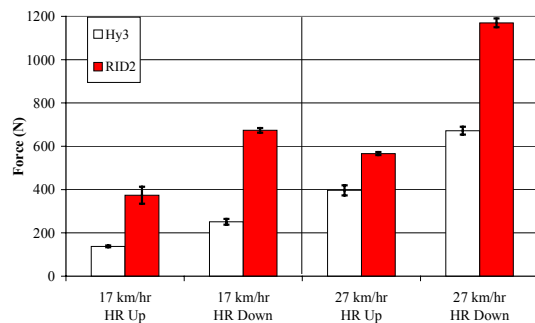


Figure 36. Series B: Lower neck tensile forces.

Occipital Condyle Extension Moments

At 17 km/hr with the head restraint full up, the peak extension moments of the Hybrid III were greater than those of the RID2 and BioRID II; however the difference between the Hybrid III and

RID2 values was less than 5 Nm. (Figure 37). At 24 km/hr with the head restraint full down, the peak BioRID moment was greater than that of the RID2, while the Hybrid III value fell between them. The extension moments of all the dummies increased with sled velocity, regardless of head restraint position. The BioRID II displayed the largest magnitude increase with sled velocity. The BioRID II response also showed the greatest increase between the head restraint full up and full down configurations at both sled velocities.

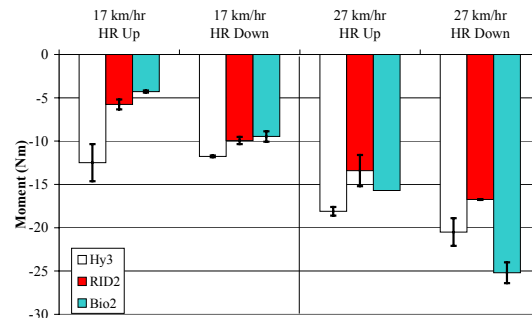


Figure 37. Series B: Occipital condyle extension moments, -My. (Note: The y-axis scale differs from that of Figure 38).

C7/T1 Extension Moments

Figure 38 shows that the C7/T1 extension moments of the Hybrid III were at least four times the RID2 values for all test conditions. The peak C7/T1 extension moments of the Hybrid III increased with sled velocity and with the change in head restraint position. The C7/T1 peak extension moments of the Hybrid III were at least three times higher than its occipital condyle moments.

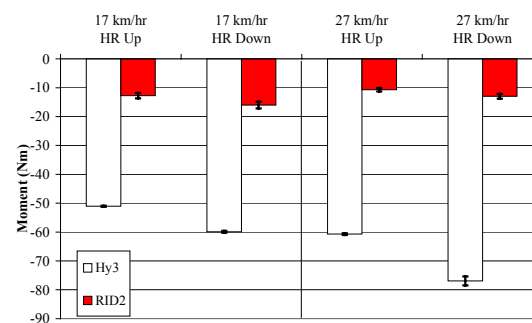


Figure 38. Series B: C7/T1 extension moments, -My. (Note: The y-axis scale differs from that of Figure 37.)

External Head Impact Fx Forces

At 17 km/hr with the head restraint full up, the external head impact Fx force of the BioRID II was

greater than that of both the Hybrid III and the RID2 (Figure 39). With the head restraint down, the Hybrid III response was lower than those of the RID2 and BioRID II. At the 27 km/hr with the head restraint down, the BioRID II peak external Fx force was lower than those of the Hybrid III and RID2. The peak external head Fx forces for all the dummies increased with sled velocity except for the BioRID II with the head restraint full down. The responses of all the dummies also increased as the head restraint was lowered, except for the BioRID II at 27 km/hr. The relatively low value of the BioRID II response in the 27 km/hr, head restraint down condition is explained by the dummy kinematics. In this condition, the head traveled over top of the head restraint, minimizing the shear force exerted on the head.

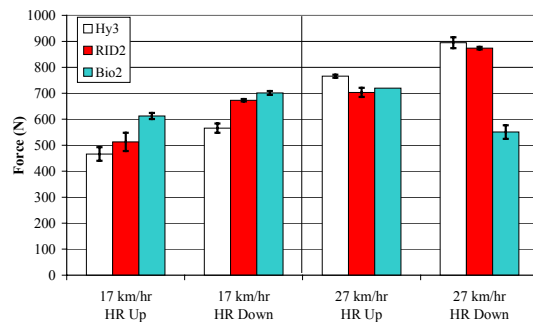


Figure 39. Series B: External head impact Fx forces.

External Head Impact Fz Forces

At 17 and 27 km/hr with the head restraint full up, the peak BioRID II Fz forces were greater than those of the Hybrid III, while the RID2 values fell between them (Figure 40). At 17 km/hr with the head restraint full down, both the BioRID II and RID2 peak Fz forces were greater than that of the Hybrid III. At 27 km/hr with the head restraint full down, the RID2 peak Fz force was greater than those of both the Hybrid III and BioRID II. Both the responses of the Hybrid III and RID2 increased with sled velocity when the head restraint was full down. The peak Fz forces for all three dummies increased when the head restraint was lowered, regardless of sled velocity. In this test series, the peak external Fz force was one of the responses most influenced by head restraint position. The peak magnitudes with the head restraint full down were 1.7 to 3.5 times greater than the peaks with the head restraint full up.

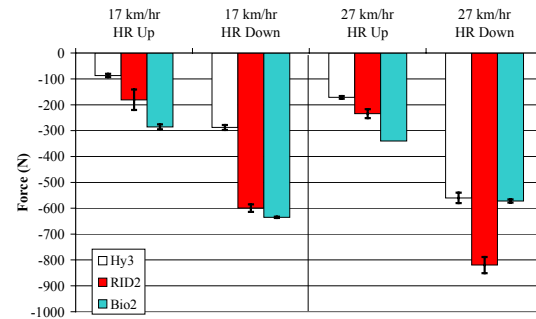


Figure 40. Series B: External head impact Fz forces.

NICs

The peak BioRID II NIC values were always greater than those of the Hybrid III and the RID2, regardless of sled velocity or head restraint position (Figure 41). At 27 km/hr with the head restraint full up, the Hybrid III also had a greater NIC than the RID2. The peak NIC values for all three dummies increased with increasing sled velocity. The NIC values did not change with head restraint position except for the RID2 and BioRID II at 27 km/hr.

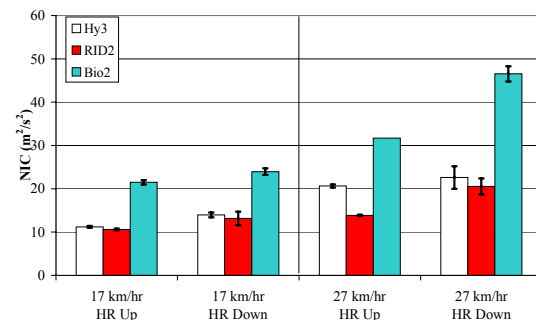


Figure 41. Series B: NICs.

In a previous evaluation program, the BioRID II was tested on rigid bench seats with no head restraints [10]. The same sled acceleration pulses were used in both programs. At the 17 km/hr ΔV , the average NIC value of the BioRID II on the rigid bench was $17.8 \text{ m}^2/\text{s}^2$ which was lower than the NIC values seen with the production seats, regardless of head restraint position. At the higher 27km/hr ΔV , the average NIC peak was 31.7 in the rigid bench seat condition. This was equivalent to the average NIC for the production seat with the head restraint full up but was still lower than the NIC with the head restraint full down. These results were counter-intuitive because the existence of a head restraint should decrease the risk of soft tissue neck injuries. However, the NIC values did not predict this, which means that the NIC may not be a good injury predictor.

Nij: Ntes

Figure 42 shows that at both sled velocities with the head restraint down, the BioRID II peak Nte values were greater than those of the Hybrid III and RID2. The peak Nte values for all three dummies increased with sled velocity and with the lower head restraint position. The BioRID II Nte peaks showed the largest change in magnitude both with sled velocity and head restraint position. For the RID2 and Hybrid III, the peak values of Nte at 17 km/hr with the head restraint full down were nearly identical to those measured at 27 km/hr with the head restraint full up.

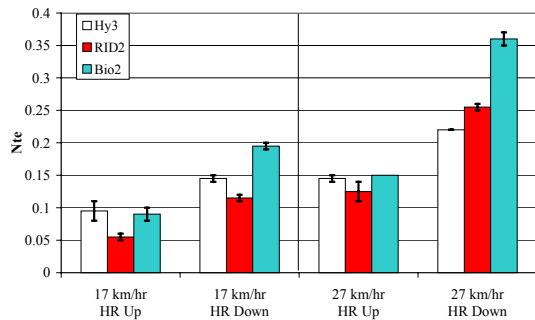


Figure 42. Series B: Ntes.

Head Restraint Contact Times

At both sled velocities with the head restraint full up, the RID2 contact times were less than those of the Hybrid III and BioRID II (Figure 43). This is attributed to the different bending stiffnesses of the dummy necks and to their different backsets (Figure 8). None of the dummies showed a change in restraint contact time with increased sled velocity. As explained in Series A, two possible factors for this may be the increased dummy/seat interaction prior to contact and the similarity of the acceleration pulses. The head restraint contact times of the RID2 increased with the lower head restraint position. The variations in these responses may be subject to the calculation method (see Methods section).

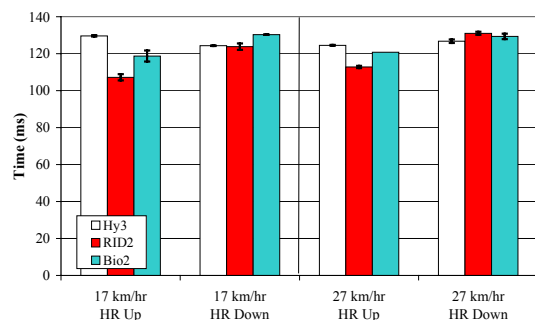


Figure 43. Series B: Head restraint contact times.

For all three dummies in Series B, the lowest peak responses were seen at the 17 km/hr ΔV with the head restraint full up. The highest peak responses occurred at the 27 km/hr ΔV with the head restraint full down. The peaks of the two other conditions, 17 km/hr with the head restraint full down and 27 km/hr ΔV with the head restraint full up, fell between those two extremes.

BioRID II: Backset Sensitivity

In one of the two 27 km/hr, head restraint full up tests, the backset of the BioRID II was 57 mm. In the other test, the backset was 83 mm. This difference in backset influenced both the measured and calculated responses, five of which are shown in Figure 44. Each individual response was normalized by its respective value at 57 mm. Another interesting point to note is the difference in the timing of the peak responses due to the change in backset. (Appendix C gives the time history curves for these responses.) At 27 km/hr, the peak responses of the 57 mm backset condition occurred on average 18 ms earlier, including a 20 ms shift in head restraint contact time, compared to the 83 mm backset responses.

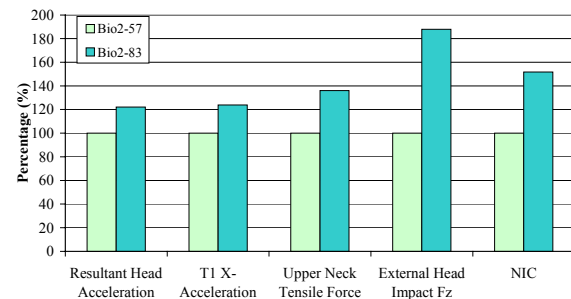


Figure 44. Series B: BioRID II backset sensitivity, 27 km/hr. Normalized responses.

SERIES C

In this series, the effect of sled velocity and the position of the head restraint on the responses of the Hybrid III and RID2 were studied. Sled tests were conducted at 10 and 24 km/hr.

Resultant Head CG Accelerations

The Hybrid III had higher peak resultant accelerations than the RID2 at 24 km/hr as shown in Figure 45. This difference may be due to the greater backset of the Hybrid III and the increased sled velocity. At 10 km/hr, this trend was not evident. The responses of both dummies increased with increasing sled velocity. The peak accelerations of the Hybrid III and the RID2 did not increase when the head restraint position was changed to full down. This may

be due to the fact that the head CGs of both dummies were below the top of the head restraint for both the full up and full down head restraint positions (Figure 13).

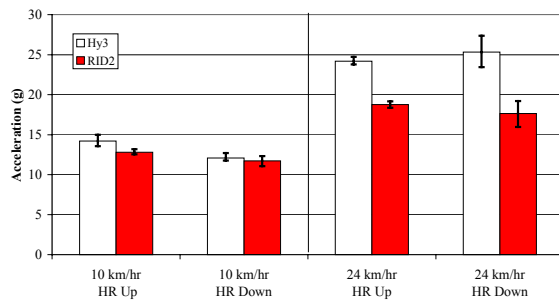


Figure 45. Series C: Resultant head CG accelerations.

T1 X-Accelerations

The T1 X-accelerations of the Hybrid III and RID2 showed the same trends as the head CG resultant accelerations. See Figure 46. The initial geometric factors, as described in the previous section, influenced the T1 X-accelerations in the same manner.

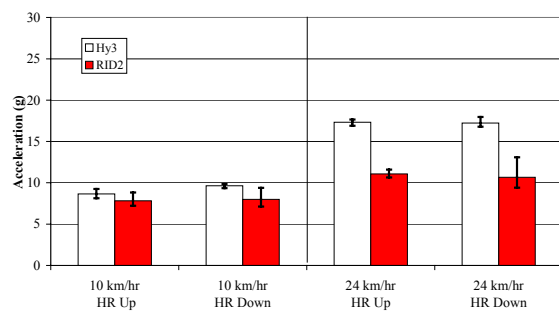


Figure 46. Series C: T1 X-accelerations.

Upper Neck Shear Forces

For both sled velocities, the Hybrid III upper neck shear forces were greater than those of the RID2 (Figure 47). This was attributed to the greater shear stiffness of the Hybrid III neck [10] and its larger backsets. The response of the Hybrid III with the head restraint full up increased with sled velocity. At the 24 km/hr ΔV with the head restraint full down, the Hybrid III peak shear force decreased as compared to the full up position. In the RID2, the upper neck shear forces were independent of sled velocity and head restraint position. This may have been due to the greater head restraint displacement at 24 km/hr as seen in Figure 48. The head restraint always deflected more in the full up position than in the full down position.

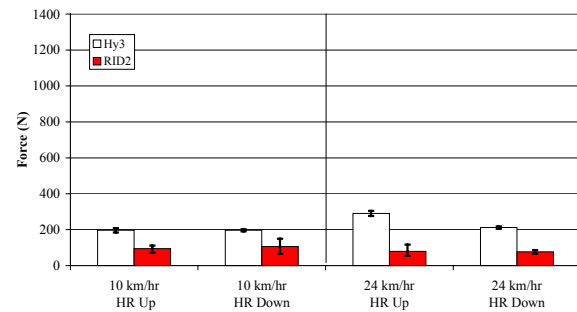


Figure 47. Series C: Upper neck shear forces, Fx.



a.)

b.)

Figure 48. Series C: Maximum head restraint deflection with the RID2 a.) 10 km/hr and b.) 24 km/hr.

Lower Neck Shear Forces

Similar to the upper neck shear forces, the Hybrid III lower neck shear forces were greater than those of the RID2 (Figure 49) for all test conditions. This was attributed to the higher stiffness of the Hybrid III thoracic spine. The Hybrid III responses almost doubled with the sled velocity increase while the RID2 responses increased by at least 15%. The lower neck shear forces of both the Hybrid III and the RID2 were at least 80% greater than their upper neck shear forces.

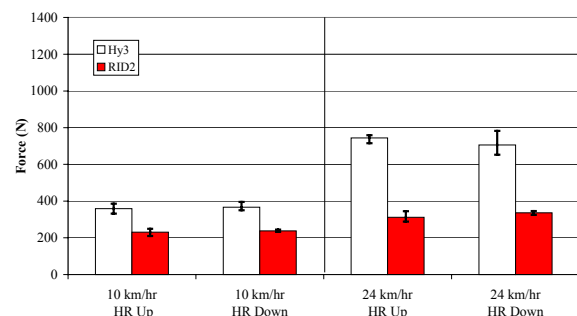


Figure 49. Series C: Lower neck shear forces, Fx.

Upper Neck Tensile Forces

In each test condition, the upper neck tensile peaks of the Hybrid III and RID2 were comparable to each other (Figure 50). The responses of both dummies increased with sled velocity by at least 80%. The upper neck tensile forces were at least double the shear forces for both dummies.

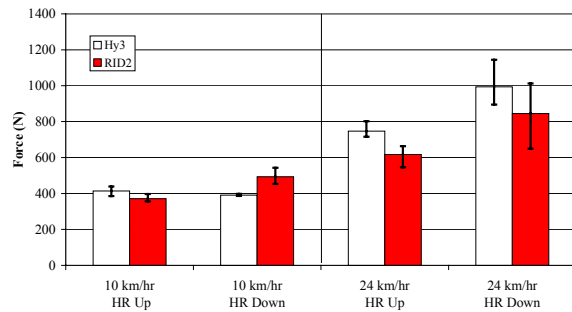


Figure 50. Series C: Upper neck tensile forces, Fz.

Lower Neck Tensile Forces

At 10 km/hr with the head restraint full down, the peak lower neck tensile forces of the RID2 were greater than those of the Hybrid III (Figure 51). With the head restraint full up, the difference between the Hybrid III and RID2 averages was less than 200 N. The Hybrid III tensile forces increased with sled velocity. The 24 km/hr RID2 lower neck axial forces were unavailable due to an instrumentation malfunction.

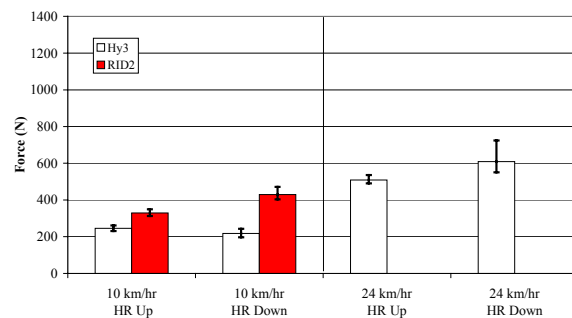


Figure 51. Series C: Lower neck tensile forces.

Occipital Condyle Extension Moments

At 24 km/hr with the head restraint full up, the peak Hybrid III extension moment was greater than that of the RID2 but the difference in the peak values was less than 5 Nm (Figure 52). In the other test conditions, the difference was even smaller and the moments were considered to be comparable. The Hybrid III extension moments increased with sled velocity, however, the magnitude change was less than 5 Nm.

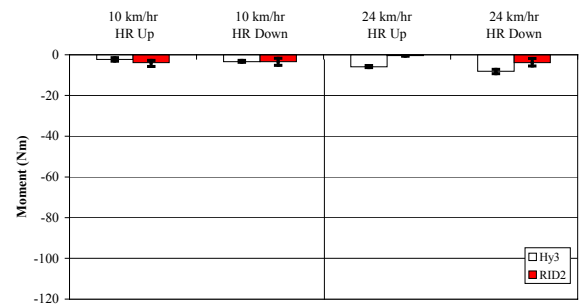
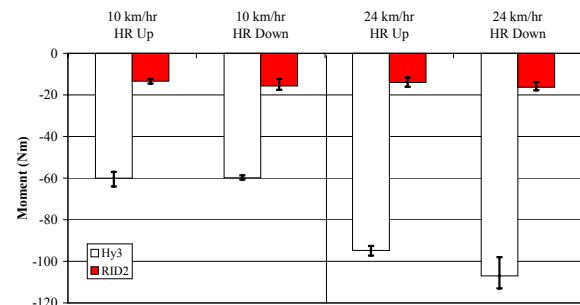


Figure 52. Series C: Occipital condyle extension moments, -My.

C7/T1 Extension Moments

The Hybrid III C7/T1 extension moments were more than three times those of the RID2 at both sled velocities (Figure 53). This was due to the higher bending stiffness of the Hybrid III neck compared to that of the RID2. The Hybrid III peak moments also increased with sled velocity. The C7/T1 peak extension moments of the Hybrid III were an order of magnitude higher than its occipital condyle moments. The RID2 C7/T1 moments were more than double its occipital condyle moments.



Figures 53. Series C: C7/T1 extension moments, -My.

External Head Impact Fx Forces

At 24 km/hr with the head restraint down, the peak Hybrid III external head impact Fx force was greater than that of the RID2 (Figure 54). In the other test conditions, the dummies' forces were comparable. Both the Hybrid III and the RID2 peaks increased with sled velocity.

External Head Impact Fz Forces

The peak external head impact Fz forces of both dummies were comparable for each test condition (Figure 55). With the head restraint full down, the Hybrid III peak forces increased with sled velocity.

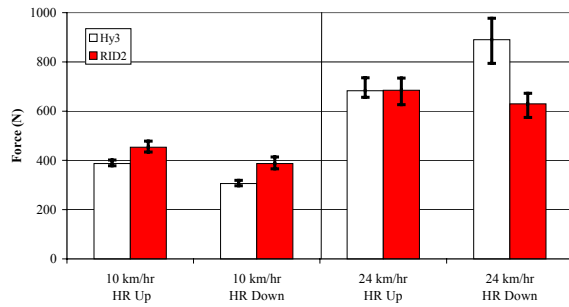


Figure 54. Series C: External head impact Fx forces.

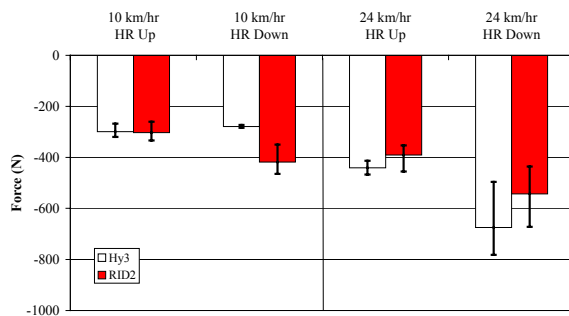


Figure 55. Series C: External head impact Fz forces.

Head Restraint Contact Times

With the head restraint in the full up position, the RID2 contacted the head restraint sooner than the Hybrid III (Figure 56). The contact times of the two dummies were more similar when the head restraint was full down. The head restraint contact times for both dummies did not change with sled velocity. Two possible reasons for this may be the increased dummy/seat interaction prior to contact, and the similar slopes of the acceleration pulses. The head restraint contact time was independent of head restraint position for both dummies.

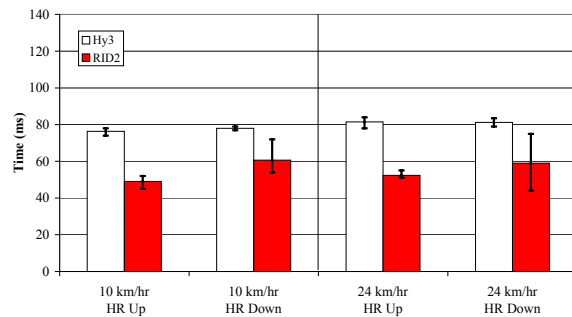


Figure 56. Series C: Head restraint contact times.

NICs

At 10 km/hr, regardless of head restraint position, and at 24 km/hr with the head restraint full down, the

Hybrid III and RID2 had similar NIC values (Figure 57). At the higher 24 km/hr ΔV with the head restraint full up, the Hybrid III peak NIC was greater than that of the RID2. Regardless of head restraint position, the Hybrid III NIC values increased with sled velocity while the RID2 NIC values did not increase.

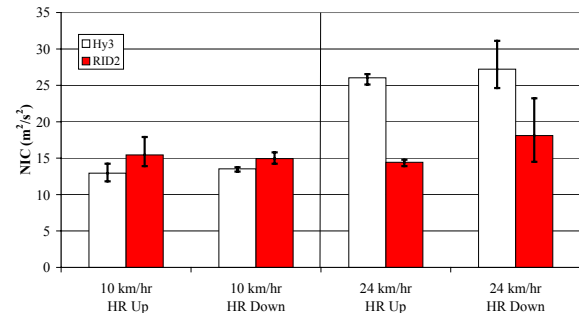


Figure 57. Series C: NICs.

Nij: Ntes

The Hybrid III and RID2 had comparable Nte values for each test condition (Figure 58). The peak Nte values of both dummies also increased with sled velocity. At 24 km/hr, the peak Nte values of both dummies increased when the head restraint was lowered.

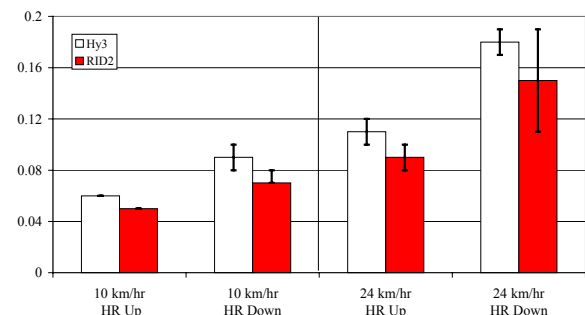


Figure 58. Series C: Ntes.

One result seen in Series C that was not seen previously was that none of the Hybrid III or RID2 responses distinguished the two head restraint positions.

Repeatability

In Series C, three repeat tests were conducted on both the Hybrid III and RID2 in each test condition. An analysis was conducted to determine the degree of repeatability of the dummy responses and how well they correlated with the impact conditions. Correlation analysis was done on the two main aspects of similarity between the repeated responses, namely, the magnitude and the characteristic shape.

Correlation coefficients with values of 1 indicate identical characteristics whereas values of 0 indicate orthogonality or lack of correlation.

Before analyzing the responses of the dummies, a coefficient of variance (CV) study was done for two test setup parameters: dummy position and sled pulse. The dummy H-point position and the peak sled pulse CVs were studied for each repeated test condition to confirm that there was minimal variation in the input. The results of that study are shown in Table 3.

Table 3.
Coefficient of Variation Table (%)

	Hybrid III				RID2			
	10 km/hr		24 km/hr		10 km/hr		24 km/hr	
	HR Up	HR Down	HR Up	HR Down	HR Up	HR Down	HR Up	HR Down
H-pt X	0.2	0.3	0.3	0.3	0.1	0.0	0.2	0.18
H-pt Z	1.8	1.4	2.3	0.5	1.2	1.9	0.4	0.54
Peak Sled Acc.	10.0	2.32	0.94	1.22	10.0	2.32	0.94	1.22

It is seen from Table 3 that the majority of the CVs were below 3%, which reflects a high degree of repeatability in the initial test setup. The peak sled pulse acceleration at 10 km/hr was the only parameter that was at 10%.

The correlation coefficients for the magnitude and shape for the majority of the measured dummy responses were computed using the formulas given by Xu et al. [25]. Due to space limitations, only the head and T1 X-acceleration responses of the Hybrid III and RID2 are presented here. The results of this analysis are shown in Figures 59-62. Appendix D, Tables D1-D4 give additional results.

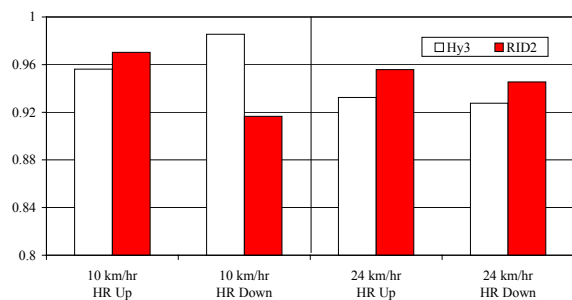


Figure 59. Magnitude correlation coefficient for the head acceleration response.

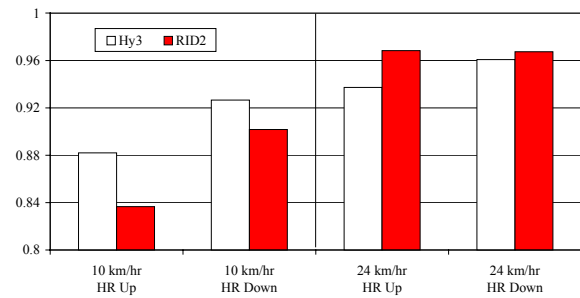


Figure 60. Magnitude correlation coefficient for the T1 X-acceleration response.

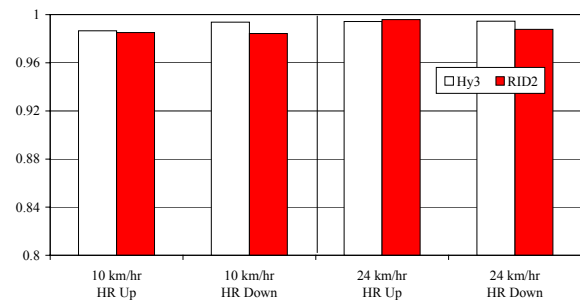


Figure 61. Shape correlation coefficient for the head acceleration response.

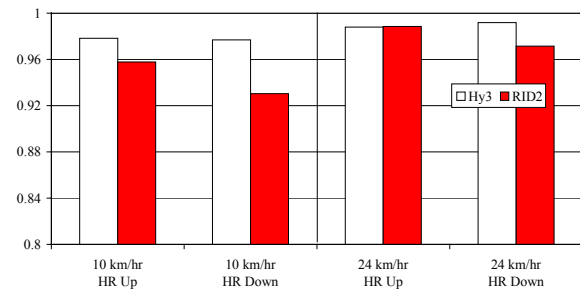


Figure 62. Shape correlation for the T1 X-acceleration response.

The repeatability of the dummy responses was classified according to Table 4.

Table 4.
Classification table for correlation coefficient

Correlation Coefficient	Classification
$0.97 \leq 1.00$	Excellent
$0.91 < 0.97$	Good
$0.00 < 0.91$	Poor

For both the Hybrid III and RID2, the bar charts show that the shape correlation coefficient values for both the head and T1 X-acceleration responses were consistently better than the magnitude values. The head had better correlation coefficients compared to the T1 for both magnitude and shape. Overall, the majority of the correlation coefficients were higher than 0.9, indicating an excellent to good degree of repeatability for both dummies. The only response with a correlation coefficient below 0.9 was the peak magnitude of T1 for the head restraint full up position at 10 km/hr. This may be attributed to the low CV value for the sled pulse in this test condition.

General Observations

In this section, any findings or trends that were observed in two or more of the test series are discussed.

Dummy Characteristics

Although all three dummies were intended to represent the 50th percentile male, their seated heights relative to the head restraint were different. In Series A, the Hybrid III head was more than 10 mm lower than that of the RID2 (Figure 5). In Series B, the Hybrid III head was at least 10 mm lower relative to the head restraint with at least 20 mm greater backset than the heads of the other two dummies, Figures 8 and 9. On the average, the head of BioRID II was consistently higher relative to the head restraint than those of the other dummies. In Series C, the vertical height measurements were not taken.

The difference in seated heights may also be explained by their designs. The Hybrid III, like the ATD 502, was designed for an automotive seated posture with an eye location that matched the 50th percentile adult male eyepoints [9, 24]. The RID2 design was revised to match the length of the WorldSID [15], and therefore matches the stature for a 50th percentile male as reported in Anthropometry of Motor Vehicle Occupants (AMVO) [22, 5]. The BioRID II was also designed to match the AMVO data [6, 22]. These differences in seated height, whether due to dummy positioning or design, may affect the way each dummy interacted with the head restraint/seat system and their responses.

One of the most noticeable differences between the Hybrid III and RID2 was the magnitudes of their C7/T1 extension moments. The Hybrid III moments were consistently at least three times greater than those of the RID2. This was due to the lower bending

stiffness of the RID2 neck and thoracic spine compared to those of the Hybrid III [10]. Throughout the series, the RID2 C7/T1 extension moments remained below 20 Nm. It should also be noted that the Hybrid III C7/T1 extension moments were at least three times greater than its occipital condyle moments. The BioRID II used in this evaluation was not equipped with a lower neck load cell; therefore, no comparison can be made.

Throughout the evaluation, there was one trend that was seen in both the Hybrid III and the RID2. The lower neck shear forces of both dummies were consistently greater than their respective upper neck shear forces by at least 35%.

A second trend that was observed was that the upper neck tensile forces of the BioRID II and RID2 were always greater than their respective upper neck shear forces. This was usually true for the Hybrid III as well; with the exception of the 8 km/hr Series A tests.

Dummy Responses to Sled Velocity

Overall, in each of the three test series, the tested dummies were found to be sensitive to sled velocity. Although there were many responses that increased as the sled velocity was increased, there were very few highly sensitive responses that were consistent across the entire evaluation. For the Hybrid III, only the lower neck tensile force increased in all three test series as the sled velocity was increased. For the RID2, it was the upper neck tensile force. The BioRID II was only tested in Series B. Its most sensitive responses were the upper neck extension moment, the Nte, and the NIC.

The head restraint contact times for each dummy, in all three test series, were insensitive to the sled velocities and acceleration pulses used in this evaluation. There are two possible contributors to this phenomenon. The first is that the dummies' interaction with the seat, as the sled velocity was increased, caused more seatback deformation prior to contact. This would move the head restraint further rearward of the dummy's head, offsetting the effect of the increased sled velocity. Another factor may be that within each test series, the sled acceleration pulses had very similar onset slopes, regardless of sled velocity, and the dummies may be reacting the same way until they contact the head restraint. The influence of these two factors may vary depending on the type of seat and sled acceleration pulses used.

With respect to the sled velocity change from 16 to 24 km/hr, the majority of the responses of the Hybrid III and RID2 did not increase in Series A.

However, at a comparable sled velocity change from 17 to 27 km/hr, the majority of the Hybrid III and RID2 responses did increase in Series B. This can be attributed to the different levels of seatback deformation between the two series.

Dummy Responses to Head Restraint Position

Series B and C both investigated the effect of head restraint position on the dummy responses. In Series B, the majority of the BioRID II, Hybrid III and RID2 responses increased when the head restraint position was changed from full up to full down. In Series C, the majority of the Hybrid III and RID2 responses did not change with head restraint position. (The BioRID II was not tested in Series C).

In Series B, when the head restraint was full up, the top of the head restraint was above the CG of the heads of all three dummies (Figure 9). When the head restraint was full down, the top of the head restraint was below the head CG. In Series C, the top of the head restraint was always above the CG of the dummies' heads, regardless if it was in the full up or full down position (Figure 13). This is illustrated in Figure 63. Once the top of the head restraint is above the CG of the dummy's head, either the Hybrid III or the RID2, increasing the height of the head restraint does not have a significant effect on the dummy responses.

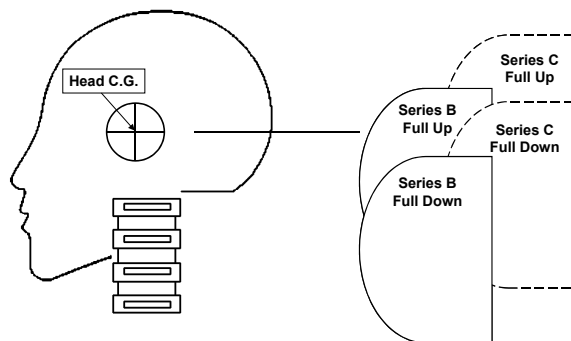


Figure 63. This graphic illustrates only the vertical height difference, relative to the CG of the head, between the full up and full down head restraint positions for Series B and C. (The backsets are not represented here).

For Series B, the external head impact Fz and the upper and lower neck tensile forces were the most sensitive Hybrid III responses to head restraint position. For the RID 2, the external head impact Fz, the Nte, and the upper neck tensile force were the three responses that increased the most when the head restraint was lowered. For the BioRID II, the

Nte, the upper neck shear force, and the external head impact Fz were the top three responses most affected by head restraint position. Across the three dummies, the external head impact Fz force was the most sensitive response to head restraint position while the T1 X-acceleration response was the least.

For Series C, none of the Hybrid III or RID2 responses distinguished between the two head restraint positions.

Backset Sensitivity

In Series A, the RID2 was tested at two different backsets: 55 and 105 mm. At the two lower sled velocities, 9 and 16 km/hr, most of the RID2 responses were insensitive to the change in backset. However, at 24 km/hr more seatback deformation occurred than at 16 km/hr, which combined with the larger backset, delayed the head restraint contact time by approximately 13 ms (Figure 25). The head gained more velocity and struck the internal structure of the head restraint (Figure 29), resulting in the majority of the RID2(105) responses increasing.

In Series B, the BioRID II was tested at 27 km/hr with backsets of 57 and 83 mm. Both the measured and calculated responses increased at the larger backset.

Handling Issues

Use of these dummies in a testing environment highlighted several areas where the dummies were already improved or could be improved further.

Hybrid III

The Hybrid III could benefit from the addition of tilt sensors to the head and pelvis regions to streamline the positioning process.

The Hybrid III is not designed for T1 target placement, requiring the test labs to fabricate something on site. Designated target locations on the lower neck would simplify this.

RID2

The lifting mechanism does not securely hold the dummy in place but allows it to slip sideways while suspended. This lifting method is difficult to use in a vehicle buck environment.

The neck positioning cable system requires improvement. It is complicated to use, difficult to adjust accurately, and also is not robust, because the cables slipped from their setting during testing and required readjustment more than once.

The neck is too soft to maintain its position in between testing, and requires a neck brace or removal of the head/neck, which is not practical for production environments. The brace that was supplied did not fit the dummy well and therefore did not provide optimal support for the neck, and also required removal of the T1 targets between consecutive tests. A system that is more customized for the dummy and easier to use is needed.

The use of tilt sensors for positioning the RID2 could streamline the positioning process, however the system provided requires some improvement. The tilt sensors should all be hard mounted in their appropriate locations to prevent slippage of the sensor inside the dummy.

BioRID II

The lifting mechanism must be removed for each test to prevent interaction with the lap belt, and the neck attachment also requires the T1 targets to be removed each time the dummy is lifted. The entire mechanism is difficult to use in a vehicle buck.

The use of a water bladder on a sled environment is a concern. Leakage could cause serious damage to sled equipment. Perhaps a fluid with a higher viscosity or gel like that used in the abdominal insert developed by Rouhana et al. [16] would minimize the damage caused by a leak.

Finally, the arm attachments do not securely attach the arms to the dummy. During sled tests the arms were seen to flail considerably, apparently causing damage to the chest jacket.

RID2 Neck Buffer Configuration

After this evaluation was completed, it was discovered that the RID2 neck buffer configuration was incorrect in both Series B and C. In Series B, the RID2 neck was missing a symmetrical pair of "D" buffers on neck level 1 (Figure 64). In Series C, a symmetrical pair of "C" buffers was missing on neck level 3 (Figure 65). To determine the effect of the missing buffers, 3 m/s pendulum tests were run with a RID2 neck that was configured as designed (correctly) and then configured to match each of the two tested configurations. Two repeat tests were conducted on each configuration in both flexion and extension. Due to the similar responses of all three neck configurations, see Appendix E, the effect of the missing buffers was judged to be negligible and does not invalidate the presented data.

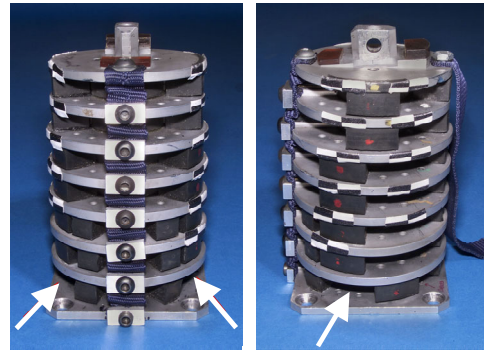


Figure 64. Series B: RID2 neck buffer configuration. The arrows point to the missing pair of "D" buffers.

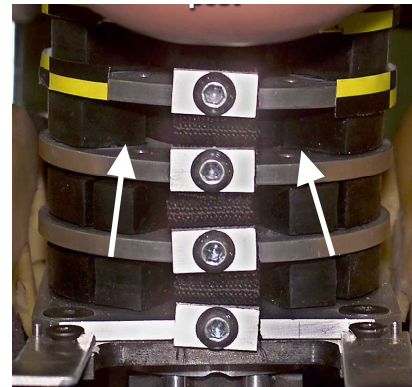


Figure 65. Series C: RID2 neck buffer configuration. The arrows point to the missing pair of "C" buffers.

CONCLUSIONS

- The C7/T1 extension moments of the Hybrid III were at least three times greater than those of the RID2. (The BioRID II was not instrumented with a lower neck load cell.)
- For the Hybrid III, the C7/T1 extension moments were at least three times its moments at the occipital condyles.
- For the Hybrid III and the RID2, the lower neck shear forces were always at least 35% greater than their respective upper neck shear forces. (The BioRID II was not instrumented with a lower neck load cell.)

- For the BioRID II and the RID2, the upper neck tensile forces were always greater than their respective upper neck shear forces.
 - For the Hybrid III, the upper neck tensile forces were usually greater than its upper neck shear forces.
- The BioRID II, Hybrid III and RID2 were all sensitive to sled velocity. (The BioRID II was only tested in Series B.)
 - The Hybrid III lower neck tensile force response was sensitive to sled velocity in all three test series.
 - The RID2 upper neck tensile force response was sensitive to sled velocity in all three test series.
- For all three dummies, the head restraint contact times were not sensitive to the sled velocity increases in these tests.
- In Series A, the seatback deformation that occurred at 24 km/hr limited the amount by which the Hybrid III and RID2 responses would have increased due to the sled velocity increase (16 to 24 km/hr) alone. (The BioRID II was not tested in Series A.)
- The BioRID II, Hybrid III, and RID2 dummies were sensitive to a head restraint position change from below their head CGs to above it.
- The Hybrid III and RID2 dummies were not sensitive to increases in head restraint height if the head restraint was already above their head CGs. (The BioRID II was not evaluated in this condition.)
- Neither the NIC nor the Nte, both of which are proposed injury criteria, provided additional information over the measured responses.
- The responses of the BioRID II and RID2 increased with larger backsets at approximate sled velocities of 24-27 km/hr.
 - At 9 and 16 km/hr, the RID2 responses were not affected by the change in backset from 55 to 105 mm. (The BioRID II was only tested at 27 km/hr.)

- As tested in Series C, both the Hybrid III and the RID2 had acceptable repeatability. (The BioRID II was not tested in this series.)

ACKNOWLEDGMENTS

The authors would like to thank Denton ATD, Inc. and Robert A. Denton, Inc. for providing the BioRID II and the necessary load cells for its use. Special thanks go to John Arthur and Mike Salloum for their technical support. We would also like to thank First Technology Safety Systems for providing the RID2 and the necessary load cells for its use and for hosting two RID2 technical sessions. Special thanks go to Steve Goldner and York Huang for their technical support. Special thanks also go to Mat Philippens, TNO Automotive, for sharing his technical expertise in support of this evaluation.

The authors would also like to thank Chris Addepalli, Charles Armstrong, Craig Hill, John Hills, James Howe, Theresa Reilly, and Kevin Taylor (DaimlerChrysler), the entire Ford SLD sled team, and Jan Morris (General Motors) for their contributions to this study.

REFERENCES

- [1] Alliance of Automobile Manufacturers. 1999. "Dummy response limit for FMVSS 208 compliance testing." Annex 2 of the Alliance of Automobile Manufacturers Submission to SNPRM, Docket No. 99-6407, December 22, 1999.
- [2] "BioRID II User's Guide." 2002. Robert A. Denton, Inc., February 27, 2002.
- [3] Boström, O., Svensson, M.Y., and Muser, M. 1999. "NIC measurement techniques and result interpretation." www.agu.ch/en/index.html, nic.calc.005.pdf.
- [4] Boström, O., Svensson, M.Y., Aldman, B., Hansson, H.A., Håland, Y., Lövsund, P., Seeman, T., Suneson, A., Säljö, A., and Örtengren, T. 1996. "A new neck injury criterion candidate- based on injury findings in the cervical spinal ganglia after experimental neck extension trauma." Proc. of 1996 International IRCOBI Conference on the Biomechanics of Impact, pp. 123-136.
- [5] Cesari, D., Compigne, S., Scherer, R., Xu, L., Takahashi, N., Page, M., Asakawa, K., Kostyniuk, G., Hautmann, E., Bortenschlager, K., Sakurai, M., Harigae, T. 2001. "WorldSID prototype dummy biomechanical responses." Stapp Car Crash Journal, 45: 285-318, 2001-22-0013.

- [6] Davidsson, J., Flogård, A., Lövsund, P., Svensson, M.Y. 1999. "BioRID P3 – design and performance compared to Hybrid III and volunteers in rear impacts at $\Delta V=7$ km/hr." Proc. of 1999 Stapp Car Crash Conference, pp. 253-265. Society of Automotive Engineers, Warrendale, PA.
- [7] Davidsson, J., Svensson, M.Y., Flogård, A., Håland, Y., Jakobsson, L., Linder, A., Lövsund, P., Wiklund, K. 1998. "BioRID I – a new biofidelic rear impact dummy." Proc. of 1998 International IRCOBI Conference on the Biomechanics of Impact, pp. 377-390.
- [8] FMVSS 208. 2000. "Occupant Crash Protection." Docket of Federal Regulations 49, Part 571.208, US Government Printing Office, Washington, D.C.
- [9] Foster, J.K., Kortge, J.O., and Wolanin, M.J. 1977. "Hybrid III – a biomechanically-based crash test dummy." Proc. 21st Stapp Car Crash Conference, pp. 973-1014. Society of Automotive Engineers, Warrendale, PA.
- [10] Kim, A., Anderson, K.F., Berliner, J., Hassan, J., Jensen, J., Mertz, H.J., Pietsch, H., Rao, A., Scherer, R., and Sutterfield, A. 2003. "A biofidelity evaluation of the BioRID II, Hybrid III and RID2 for use in rear impacts." Stapp Car Crash Journal 47: 489-523.
- [11] Mertz, H.J., and Prasad, P. 2000. "Improved neck injury risk curves for tension and extension moment measurements of crash dummies." Stapp Car Crash Journal 44: 59-75.
- [12] Mertz, H.J., Prasad, P., and Irwin, A.L. 1997. "Injury risk curves for children and adults in frontal and rear collisions." Proc. 41st Stapp Car Crash Conference, pp. 13-30. Society of Automotive Engineers, Warrendale, PA.
- [13] NHTSA. 2000. "Final rule on advanced airbags." Federal Register (FR), Vol. 65, 30680, May 12, 2000.
- [14] NHTSA. 1998. "Notice of proposed rule making (NPRM) for advanced airbags." Federal Register (FR), Vol. 63, No. 181, September 18, 1998.
- [15] Philippens, M.M.G.M. 2002. "RID2 v0.0 User Manual Draft." TNO Automotive, TNO report 01.OR.BV.048.1/MP, March 12, 2002.
- [16] Rouhana, S.W., Elhagediab, A.M., Walbridge, A., Hardy, W.N., and Schneider, L.W. 2001. "Development of a reusable, rate-sensitive abdomen for the Hybrid III family of dummies." Stapp Car Crash Journal, Vol. 45: 33-59.
- [17] SAE EA 23. 1998. "User's Manual for the 50th Percentile Male Hybrid III Test Dummy." Society of Automotive Engineers, Warrendale, PA.
- [18] SAE J1733. 1994. "Sign Convention for Vehicle Crash Testing." Society of Automotive Engineers, Warrendale, PA.
- [19] SAE J211. 1995. "Instrumentation for impact test – part 1 – electronic instrumentation." Society of Automotive Engineers, Warrendale, PA.
- [20] SAE J2052 1997. "Test Device Head Contact Duration Analysis." Society of Automotive Engineers, Warrendale, PA.
- [21] SAE PT-44. 1994. "Hybrid III: the first humanlike crash test dummy." Society of Automotive Engineers, Warrendale, PA.
- [22] Schneider, L.W., Robbins, D.H., Pflüg, M.A., Snyder, R.G. 1983. "Development of anthropometrically based design specifications for an advanced adult anthropomorphic dummy family. Volume 1 (3)." U.S. Department of Transportation, National Highway Traffic Safety Administration, report No. DOT-HS-806-715 and UMTRI-83-53-1.
- [23] Svensson, M.Y., Boström, O., Davidsson, J., Hansson, H.-A., Håland, Y., Lövsund, A., and Säljö, A. 2000. "Neck injuries in car collisions – a review covering a possible injury mechanism and the development of a new rear-impact dummy." Accident Analysis & Preventions 32: 167-175.
- [24] Tennant, J., Jensen, R., Potter, R. 1974. "GM-ATD 502 Anthropomorphic Dummy – Development and Evaluation." SAE746030.
- [25] Xu, L., Agaram, V., Rouhana, S., Hultman, R.W., Kostyniuk, G.W., McCleary, J., Mertz, H., Nusholtz, G.S., Scherer, R. 2000. "Repeatability evaluation of the pre-prototype NHTSA advanced dummy compared to the Hybrid III." Society of Automotive Engineers, Warrendale, PA. SAE 2000-01-0165.

APPENDIX A. EQUATIONS FOR CALCULATED RESPONSES

1. MOMENT TRANSFER EQUATION AND DISTANCES

$$M_{YCor} = M_Y + (F_X \bullet D_Z) + (F_Z \bullet D_X)$$

where F_X , F_Z , and M_Y are the measured loads and torques [17, 18].

Table A1.
**Correction distances for the BioRID II,
Hybrid III, and RID2**

	D _X (mm)	D _Z (mm)
Occipital Condyle: BioRID II, Hybrid III, RID2	0.0	-17.8
C7/T1: Hybrid III	50.8	28.6
C7/T1: RID2	0.0	18.0

2. EXTERNAL HEAD FORCE EQUATIONS [20][†]

To calculate the inertia loads on the head (using a 50th percentile head mass, M = of 4.2 kg*):

$$F_{X\text{inertialload}} = M \cdot A_{X\text{head}}$$

$$F_{Z\text{inertialload}} = M \cdot A_{Z\text{head}}$$

To calculate the external head forces:

$$F_{X\text{head}} = F_{X\text{inertialload}} - F_{X\text{upperneck}}$$

$$F_{Z\text{head}} = F_{Z\text{inertialload}} - F_{Z\text{upperneck}}$$

[†]The measured head CG accelerations and the measured upper neck loads were used to calculate the external head forces, not the corrected responses.

*4.2 kg represents the mass of the head above the measurement strain gage in the upper neck load cell.

3. NIC [23, 3, 4]

$$\text{NIC} = (0.2 \cdot a_{\text{rel}}) + (v_{\text{rel}})^2$$

where $a_{\text{rel}} = T1a_x - C1a_x$,
 $v_{\text{rel}} = \int a_{\text{rel}} dt$,
 $T1a_x$ – T1 X-acceleration,
 $C1a_x$ – C1 X-acceleration[†].

[†]The head CG X-acceleration was used for C1a_x.

4. Nij - Nte [13, 14, 1, 11, 12]

$$Nte = (F_z/F_{Zc}) + (M_{OCY}/M_{Yc})$$

where $F_{Zc} = 6806 \text{ N}$ for tension and
 $M_{Yc} = 135 \text{ Nm}$ for extension.

APPENDIX B. RID2 TILT SENSOR READINGS AT INITIAL POSITION

Table B1.
Series A: RID2 55 mm backset

	Tilt Sensor 7 Head (Degree)	Tilt Sensor 6 T1 (Degree)	Tilt Sensor 5 Neck Bracket (Degree)	Tilt Sensor 3 Lumbar Bracket, Top (Degree)	Tilt Sensor 1 Lumbar Bracket, Left-Right (Degree)	Pelvic Reading* * (Degree)
9 km/hr, 1	0	6	-11	-1	-1	82.0
9 km/hr, 2	-1	6	-11	-1	0	83.9
16 km/hr, 1	-1	4	-9	-3	1	83.9
16 km/hr, 2	-1	6	-11	-1	0	83.2
24 km/hr, 1	1	6	-11	1	0	82.6
24 km/hr, 2	-1	6	-11	-1	0	83.0

*Tilt sensor 2 (Lumbar Bracket Bottom) and tilt sensor 4 (T12) were inoperative; the readings were not included.

**The pelvic angle was measured manually due to tilt sensor 2 being inoperative. A pelvic reading of 83° corresponded to 22.5°.

Table B2.
Series A: RID2 105 mm backset

	Tilt Sensor 7 Head (Degree)	Tilt Sensor 6 T1 (Degree)	Tilt Sensor 5 Neck Bracket (Degree)	Tilt Sensor 3 Lumbar Bracket, Top (Degree)	Tilt Sensor 1 Lumbar Bracket, Left-Right (Degree)	Pelvic Reading** (Degree)
9 km/hr, 1	2	12	-17	-9	0	82.6
9 km/hr, 2	1	12	-17	-5	1	83.8
16 km/hr, 1	1	12	-17	-7	-1	82.0
16 km/hr, 2	1	12	-17	-8	1	82.5
24 km/hr, 1	1	12	-17	-7	-1	83.0
24 km/hr, 2	1	12	-17	-7	0	83.8

*Tilt sensor 2 (Lumbar Bracket Bottom) and tilt sensor 4 (T12) were inoperative; the readings were not included.

**The pelvic angle was measured manually due to tilt sensor 2 being inoperative. A pelvic reading of 83° corresponded to 22.5°.

Table B3.
Series B: RID2

	Tilt Sensor 7 Head (Degree)	Tilt Sensor 6 T1 (Degree)	Tilt Sensor 5 Neck Bracket (Degree)	Tilt Sensor 3 Lumbar Bracket, Top (Degree)	Tilt Sensor 2 Lumbar Bracket, Bottom (Degree)	Tilt Sensor 1 Lumbar Bracket, Left-Right (Degree)
17 km/hr, HR up 1	-1	5	-1	-9	-1	0
17 km/hr, HR up 2	-1	2	-2	-10	1	0
17 km/hr, HR down 1	-1	5	-2	-10	1	0
17 km/hr, HR down 2	-1	4	-1	-10	0	0
27 km/hr, HR up 1	1	1	-2	-9	1	0
27 km/hr, HR up 2	-1	5	-1	-10	1	0
27 km/hr, HR down 1	0	3	-4	-9	0	0
27 km/hr, HR down 2	2	3	-2	-10	1	0

*Tilt sensor 4 (T12) was inoperative; the readings were not included.

Table B4.
Series C: RID2

	Tilt Sensor 7 Head (Degree)	Tilt Sensor 6 T1 (Degree)	Tilt Sensor 5 Neck Bracket (Degree)	Tilt Sensor 4 T12 (Degree)	Tilt Sensor 3 Lumbar Bracket, Top (Degree)	Tilt Sensor 2 Lumbar Bracket, Bottom (Degree)	Tilt Sensor 1 Lumbar Bracket, Left- Right (Degree)
10 km/hr, HR up 1	0	1	-2	1	13	-1	1
10 km/hr, HR up 2	0	0	-2	2	1	1	1
10 km/hr, HR down 1	0	-1	-1	-1	6	2	1
10 km/hr, HR down 2	0	1	-2	0	6	2	0
10 km/hr, HR up 3	0	1	-3	1	6	2	1
10 km/hr, HR down 3	1	0	-2	2	-1	2	1
24 km/hr, HR up 1	-1	0	-2	3	-1	-1	1
24 km/hr, HR down 1	0	1	-2	1	7	0	0
24 km/hr, HR up 2	0	1	-2	2	3	0	1
24 km/hr, HR up 3	0	-1	-1	0	3	1	1
24 km/hr, HR down 2	0	0	-1	1	1	1	1
24 km/hr, HR down 3	0	1	-2	0	0	2	0

APPENDIX C. SERIES B: BIORID II BACKSET SENSITIVITY TIME HISTORY RESPONSES.

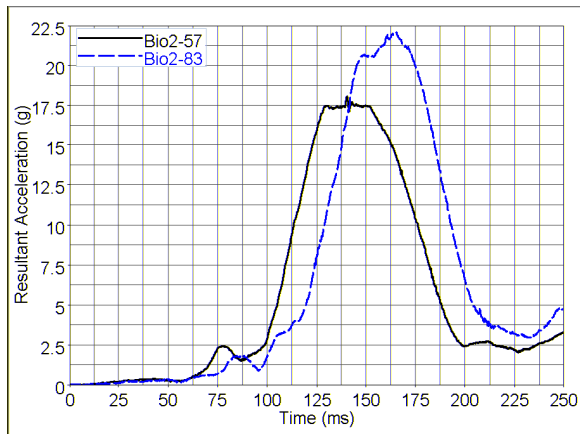


Figure C1. Series B: Resultant head acceleration. BioRID II at backsets of 57 and 83 mm.

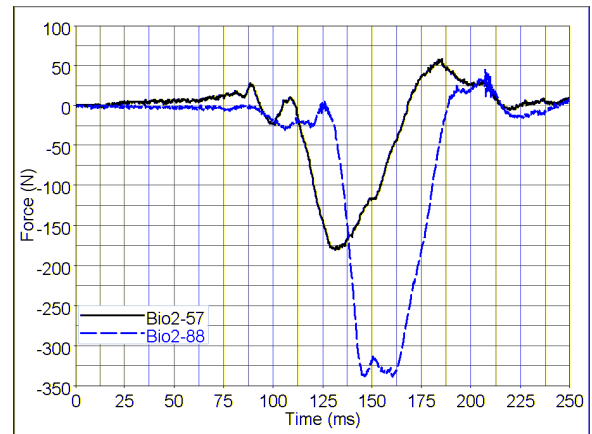


Figure C4. Series B: External head impact Fz. BioRID II at backsets of 57 and 83 mm.

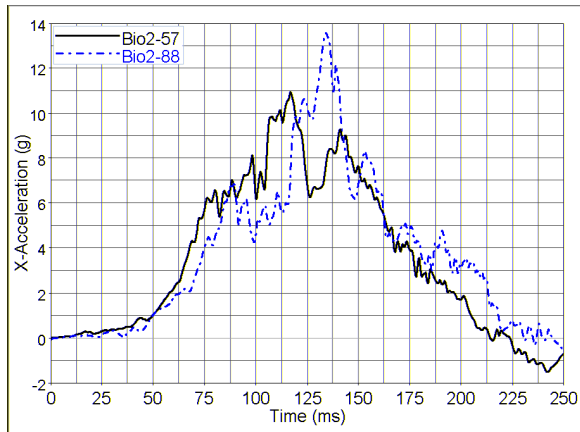


Figure C2. Series B: T1 X-acceleration. BioRID II at backsets of 57 and 83 mm.

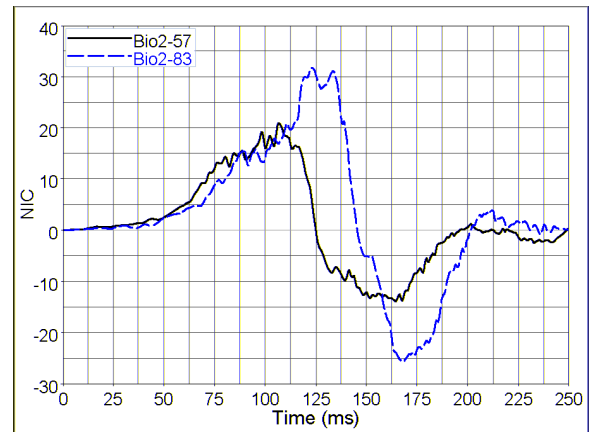


Figure C5. Series B: NIC. BioRID II at backsets of 57 and 83 mm.

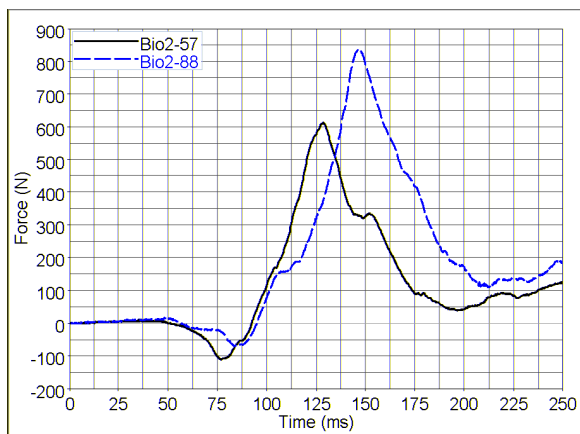


Figure C3. Series B: Upper neck Fz. BioRID II at backsets of 57 and 83 mm.

APPENDIX D. SERIES C: CORRELATION COEFFICIENTS.

Table D1.
Correlation coefficients for 10 km/hr, head restraint up

	Hybrid III			RID2		
	Magnitude	Shape	Phase	Magnitude	Shape	Phase
Head X-acceleration	0.9562	0.9866	1.4167	0.9704	0.9852	1.9
T1 X-acceleration	0.882	0.9783	2.5333	0.8366	0.9578	0.7833
T12 X-acceleration	0.8803	0.9929	2.1	0.9107	0.9478	0.35
Pelvis X-acceleration	0.9441	0.9953	2.3167	0.9386	0.9873	1.000

Table D2.
Correlation coefficients for 10 km/hr, head restraint down

	Hybrid III			RID2		
	Magnitude	Shape	Phase	Magnitude	Shape	Phase
Head X-acceleration	0.9855	0.9938	0.7667	0.9166	0.9844	0.4167
T1 X-acceleration	0.9266	0.9769	1	0.9017	0.9304	2.0667
T12 X-acceleration	0.9704	0.9727	1.3167	0.8590	0.9360	2.4833
Pelvis X-acceleration	0.8990	0.979	1.7167	0.9315	0.9826	8.5333

Table D3.
Correlation coefficients for 24 km/hr, head restraint up

	Hybrid III			RID2		
	Magnitude	Shape	Phase	Magnitude	Shape	Phase
Head X-acceleration	0.9324	0.9943	1.0833	0.9558	0.9959	2.600
T1 X-acceleration	0.9372	0.9880	1.8500	0.9684	0.9886	2.1167
T12 X-acceleration	0.9472	0.9858	1.5333	0.9145	0.9774	2.1168
Pelvis X-acceleration	0.9488	0.9877	4.0167	0.9659	0.9929	3.3833

Table D4.
Correlation coefficients for 24 km/hr, head restraint down

	Hybrid III			RID2		
	Magnitude	Shape	Phase	Magnitude	Shape	Phase
Head X-acceleration	0.9276	0.9946	0.2	0.9455	0.9879	4.8
T1 X-acceleration	0.9607	0.9918	0.0167	0.9674	0.9715	1.6167
T12 X-acceleration	0.9186	0.9910	0.2	0.9535	0.9751	2.1167
Pelvis X-acceleration	0.9205	0.9899	0.95	0.9521	0.9913	1.95

APPENDIX E. RID2 NECK BUFFER CONFIGURATION HEAD/NECK PENDULUM TESTS

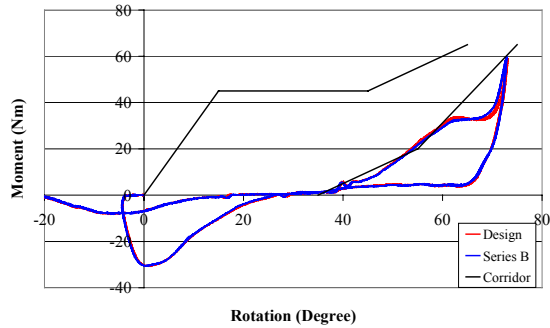


Figure E1. RID2 neck buffer configurations: Design and Series B. Flexion tests: Occipital condyle moment vs head/pendulum rotation.

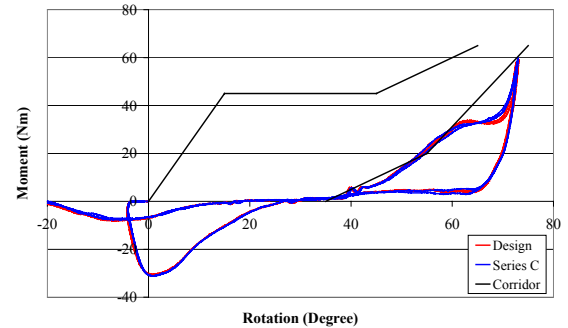


Figure E3. RID2 neck buffer configurations: Design and Series C. Flexion tests: Occipital condyle moment vs head/pendulum rotation.

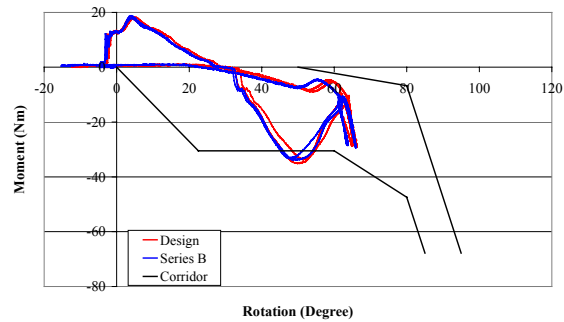


Figure E2. RID2 neck buffer configurations: Design and Series B. Extension tests: Occipital condyle moment vs. head/pendulum rotation.

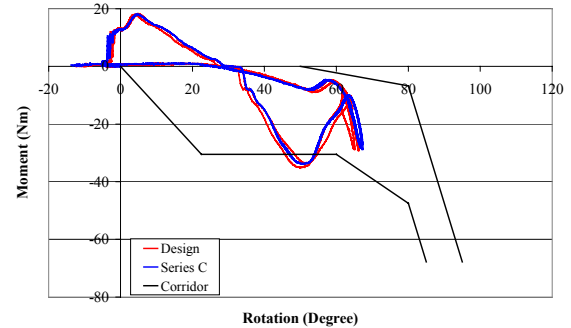


Figure E4. RID2 neck buffer configurations: Design and Series C. Extension tests: Occipital condyle moment vs head/pendulum rotation.